NGU Report 2006.082

3D modelling of gravity and magnetic data in the Trøndelag Platform

Geological Survey of Norway
NO-7491 Trondheim, Norway
Tel.: 47 73 90 40 11
Telefax 47 73 92 16 20

REPORT

Report no.: 2006.082	ISSN 0800-3416	Grading: Confidential to 31.12.2008

Title: 3D modelling of gravity and magnetic data in the Trøndelag Platform

Authors: Jörg Ebbing, Per Terje Osmundsen, Christophe Pascal	Client: Statoil ASA
County:	Commune:
Map-sheet name (M=1:250.000)	Number of pages: 50 Price (NOK): Map enclosures:

Fieldwork carried out:	Date of report: 18.12.2006	Project no.: 3144.00	Person responsible: Odleiv Olesen

Summary:

The report presents a 3D model of the entire mid-Norwegian margin, with special emphasis on the Trøndelag Platform. Based on the interpretation of OBS profiles, long-offset seismic reflection and petrophysical data the crustal structure was modelled. Seismic horizons provided by Statoil were used to refine the model in the area of the Trøndelag Platform.

Metamorphic core complexes can be observed along the entire mid-Norwegian margin sector and are especially visible in the magnetic field. The modelling reveals that the basement can be divided in a highly magnetic lower part and a less magnetic upper part, which can generally be correlated to Precambrian and Caledonian basement, respectively. Onshore-offshore interpretations on the Trøndelag Platform indicate that the late-Caledonian detachment zones control the distribution of the core complexes and the distribution of the less magnetic Caledonian upper basement nappes.

3D modelling of the highly magnetic metamorphic core complexes reveals further that the thickness and depth distribution of the high-magnetic lower basement controls the magnetic anomalies on the mid-Norwegian margin. The low amplitudes on the outer Vøring margin are hence, controlled by the structural style of the basement and not by shallow depth to the Curie temperature.

The Trøndelag Platform is clearly visible as an area with increased basement thickness compared to the other Norwegian Sea areas. Hereby, the thickness of the lower basement is correlating with the extension of the Trøndelag Platform, while the upper basement thins out in the areas of the core complexes.

Keywords: Geophysics	Continental Shelf	Research
Gravimetry	Magnetometry	3D modelling
Report		

CONTENTS

1 INTRODUCTION

We present in this report the crustal structure of the mid-Norwegian margin with special focus on the Trøndelag Platform. By 3D forward modelling of gravity and magnetic field considering a wealth of constraining information, we were able to model the crustal structure of this area and to map and characterize the basement. Herby, especially the role of the lower basement and magnetic highs observed on the Trøndelag Platform are important to identify the connection between the overlying less magnetic nappe structures and the underlying, generally high-magnetic basement.

The study is based on work performed within a variety of previous NGU projects (Ebbing et al. 2006; Olesen et al. 2002, 2003, 2004, 2006a,b; Osmundsen et al. 2002, 2006; Skilbrei et al. 2002;). While the potential field studies in these projects mainly concentrated on the outer Vøring or the Lofoten margin, the present study is presenting (1) a regional 3D model of the entire Møre-Vøring-Lofoten margin segments, and (2) a detailed 3D picture of the Trøndelag Platform.

For the Trøndelag Platform, we could make use of new, hitherto unpublished OBS data (Raum & Mjelde, pers. comm.) and information from Statoil about selected seismic horizons. Following tests of the 3D density and magnetic model against seismic depth-models, we have produced a series of updated maps displaying Top upper basement, Top lower basement (i.e. top high-density and high-magnetic basement), lower crustal bodies and Moho depth. The derived maps, the 3D density model, and the magnetic response are integrated in our discussion of deep and basement internal structures.

We will present the main structural elements of the mid-Norwegian margin Ch. 2, and the available data for our study in Ch. 3. In Ch. 4 the 3D modelling and the structural maps of the study area are presented. Ch. 5 and 6 give a tectonic synthesis and a recommendation for further work.

2 MAIN STRUCTURAL ELEMENTS IN THE STUDY AREA

The Vøring Margin has been extensively studied by the use of multi-channel seismic reflection data, seismic refraction data, commercial drilling on the continental shelf as well as scientific drilling (e.g. Planke et al. 1991, Skogseid et al. 1992, Doré et al. 1999, Brekke 2000, Mjelde et al. 2001, Raum et al. 2002, Mjelde et al. 2003 a, b, c, 2005).

The Vøring margin is located between 64° and 68° N, off Norway, and comprises three main geological provinces: the Trøndelag Platform, the Vøring Basin and the Vøring Marginal High (Figs. 2.1 & 2.2). These segments are further separated by NE-SW striking faults systems, developed since late Caledonian time. Northward the Vøring Margin is bounded by the Bivrost Lineament, representing the transition to the Lofoten Margin, while the East Jan Mayen Fracture Zone and the Jan Mayen lineament represent the southern boundary and represents the transition to the Møre Margin.

Investigating the transitional areas between the different margin segments (Møre, Vøring, and Lofoten) helps to understand the role and presence of the supposed tectonic lineaments. The definition of the lineaments is supposed to be guided primarily by changes in the structure and composition in the basement and lower crust (Mjelde et al. 2005). In this sense the lineaments can represent crustal scale shear zones or detachments.

Early Tertiary continental break-up and initial seafloor spreading between Eurasia and Greenland was characterized by massive emplacement of magmatic rocks (e.g. Eldholm and Grue 1994). On the Vøring Margin these rocks were partially extruded on the surface as flood basalts and partially intruded as sills into the sedimentary rocks in the Vøring Basin and presumably into continental crust (Mjelde et al. 2001). On the Vøring margin a lower crustal body with P-velocities and densities can be found (e.g. Mjelde et al. 2005).

We refer to this layer as lower crustal body (LCB). The LCB is not evenly distributed along the margin and is often referred to as magmatic underplating (e.g. Skogseid et al. 1992; van Wijk et al. 2004; Mjelde et al. 2005). However, while the high velocity/high density of the LCB may be considered as an objective observation, its origin as a layer of underplated material is an interpretation that dates back to work by e.g. White et al. (1987). Currently there is a renewed discussion about the interpretation of the LCB (e.g. Gernigon et al. 2003; Mjelde et al. 2005, Ebbing et al. 2006). Determining the nature of the LCB is clearly relevant for the thermal history of volcanic margins, and arguably also for the entire concept of the development of such margins.

The Trøndelag Platform forms the innermost, landward part of the Vøring margin system (Fig. 2.1). The Trøndelag Platform has been a relatively stable area since the Jurassic and it is covered by relatively flatlying and mostly parallel-bedded strata which usually dip gently northeastwards (Blystad et al. 1995). Within the area of the Trøndelag Platform several sub-units can be found like the Nordland Ridge, Helgeland Basin, Frøya High and Froan Basin.

The Halten Terrace is separated from the Trøndelag Platform to the east by the Bremstein Fault Complex, and from the Frøya High to the southeast by the Vingleia Fault Complex. The Halten Terrace was separated from the Trøndelag Platform during the Neocomian, after the deep erosion of the uplifted western margin of the early platform (Frøya High, and Sklinna and Nordland Ridges).

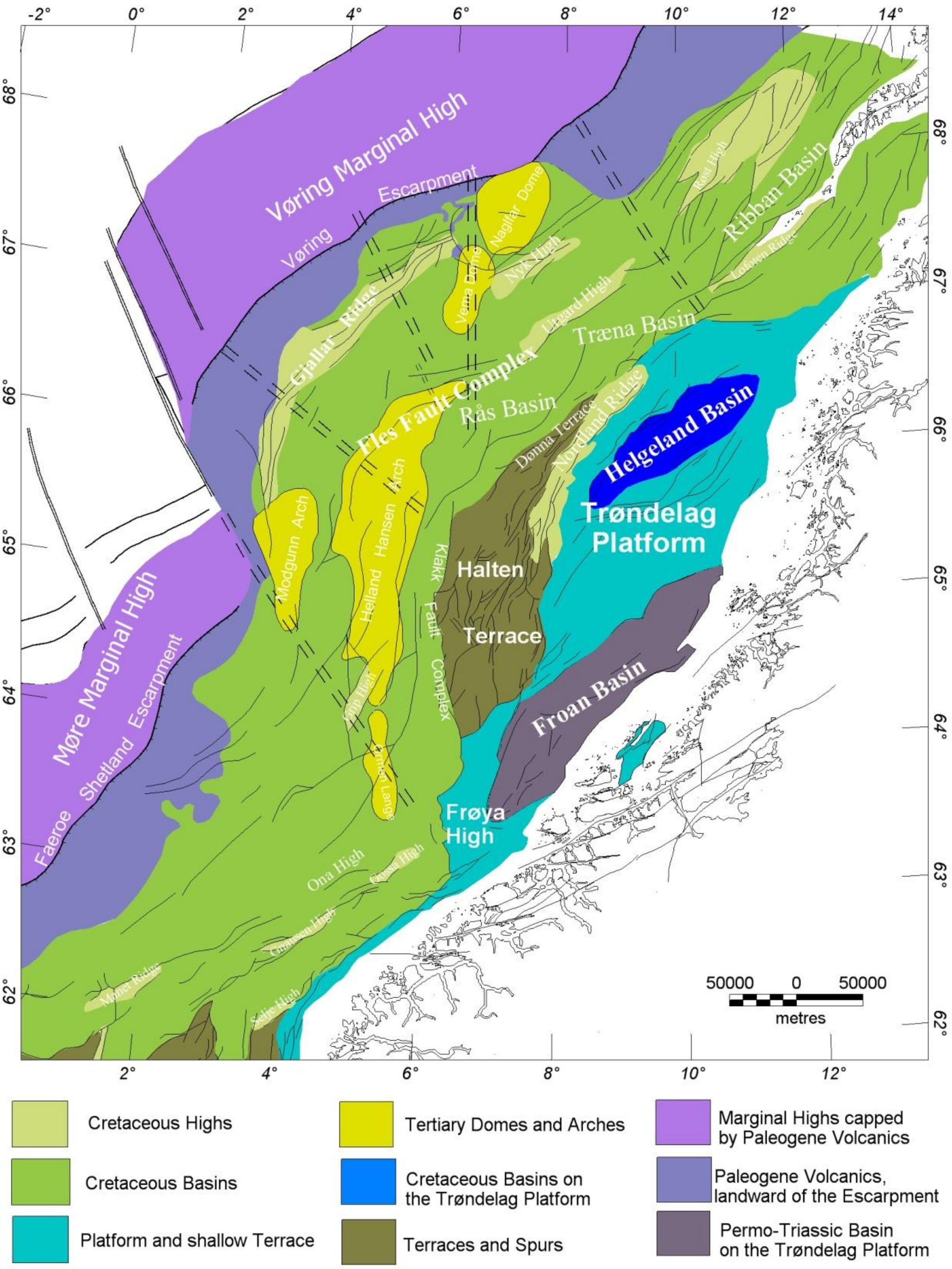

Figure 2.1 *Tectonic setting of the mid-Norwegian margin (after Blystad et al. 1995).*

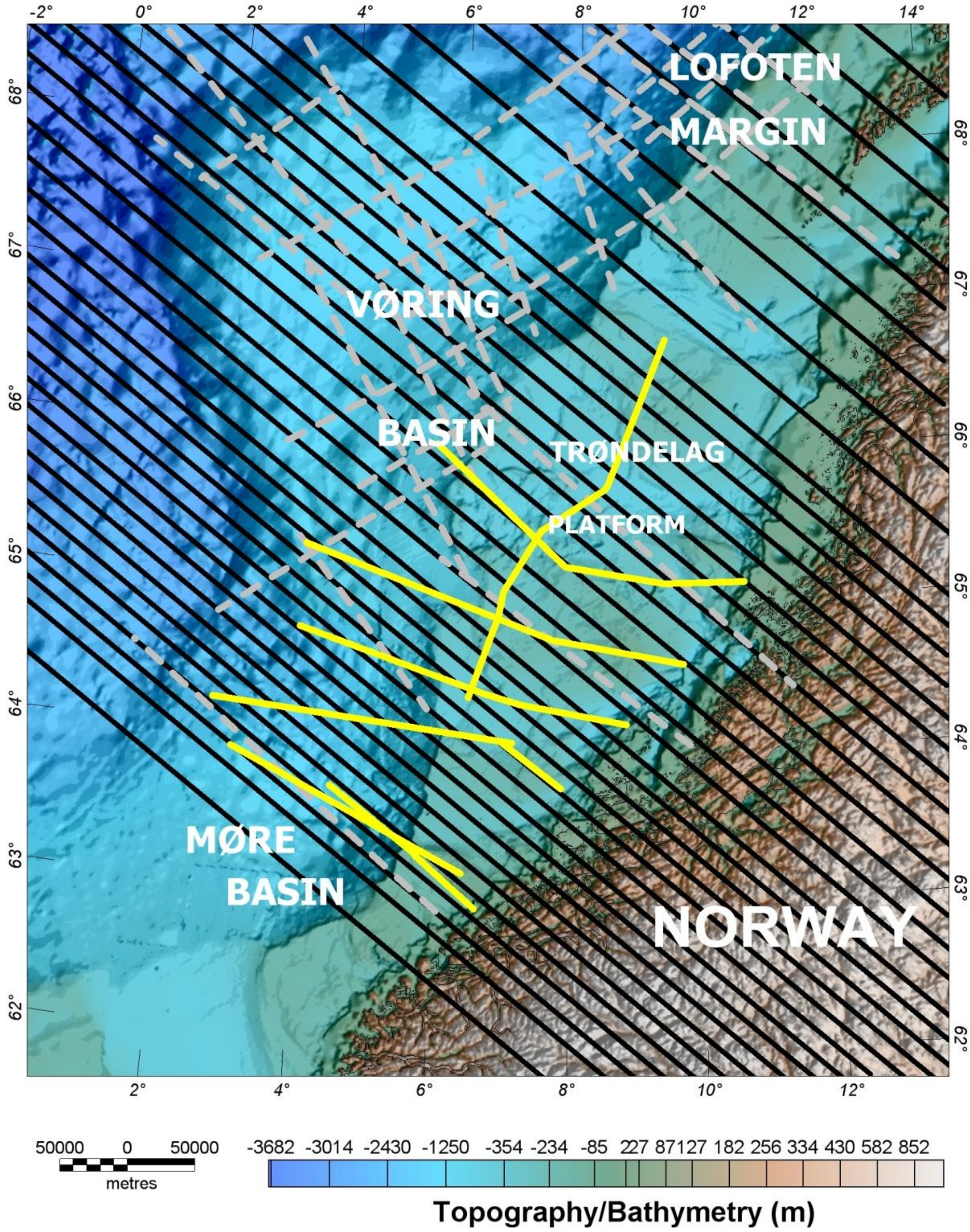

Figure 2.2 *Bathymetry of the mid-Norwegian margin. The bathymetric data are from a compilation by Dehls et al. (2000), which is based on satellite altimeter data released by Smith & Sandwell (1997) for the deep-water part of the study are, and data provided by the Norwegian Mapping Authority, Marine Department Stavanger for the shallow water areas. The grey dotted lines in (a) mark the location of the OBS profiles (see Mjelde et al. 2005 for more details), while the thin black lines indicate the cross-sections of the 3D density model. Yellow lines show the long-offset profiles after Osmundsen et al. (2006).*

3 DATA SETS

3.1 Gravity data

Gravity data were compiled by Skilbrei et al. (2000) from gravity stations on mainland Norway in addition to marine gravity data from the Geological Survey of Norway, the Norwegian Mapping Authority, the Norwegian Petroleum Directorate and Norwegian and foreign universities and commercial companies. The compiled grid was merged with gravity data from satellite altimetry in the deep-water areas (Andersen & Knudsen 1998). The compiled free-air dataset has been interpolated to a square grid of 2 km x 2 km using the minimum curvature method (Geosoft 2005). The simple Bouguer correction at sea (Mathisen 1976) was carried out using the bathymetry data in Figure 2.2 and a density of 2200 kg/m^3. The International Standardization Net 1971 (I.G.S.N. 71) and the Gravity Formula 1980 for normal gravity have been used to level the surveys. Figure 3.1 and 3.2 show the gravity anomaly and the Bouguer anomaly, while the location of the gravity stations and the marine profiles are shown in Figure 3.3.

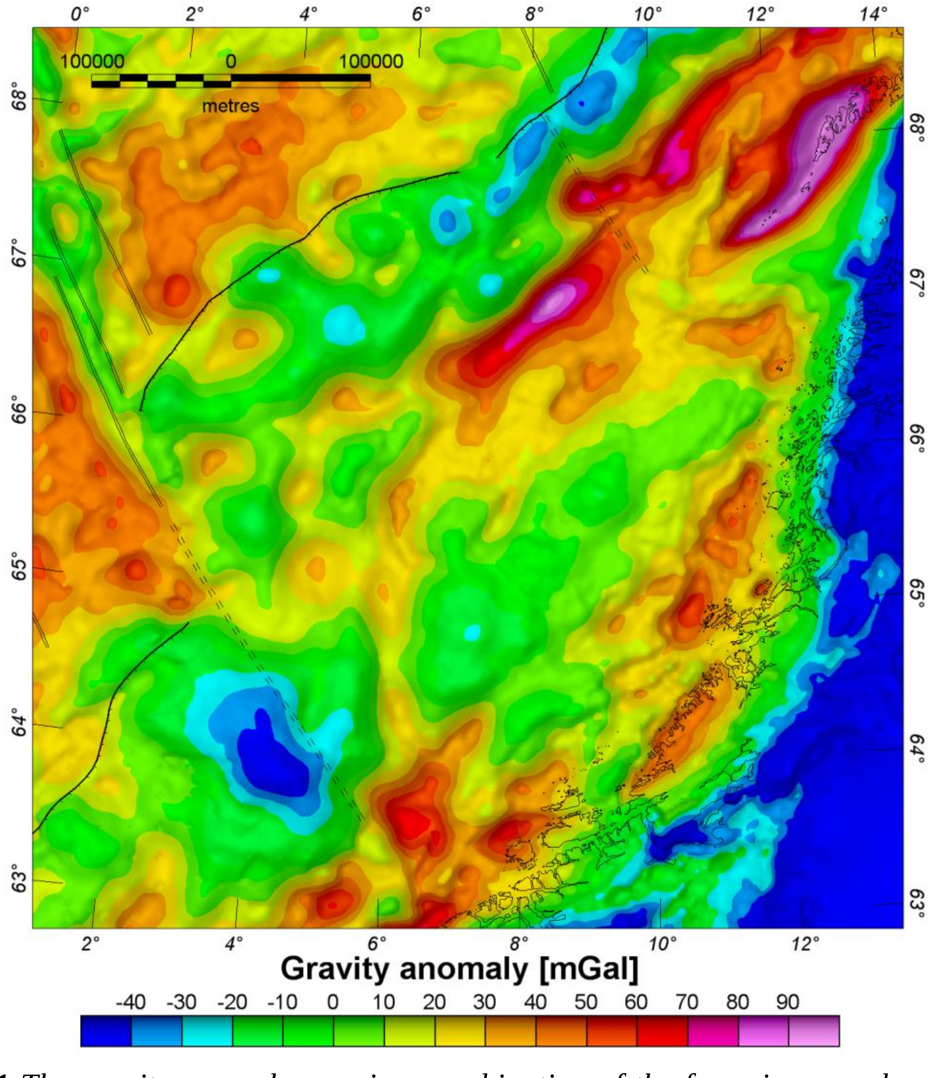

Figure 3.1 *The gravity anomaly map is a combination of the free-air anomaly offshore and the Bouguer anomaly onshore (modified from Skilbrei et al. 2000). Offshore measurements of approximately 59,000 km of marine gravity profiles have been acquired by the Norwegian Petroleum Directorate, oil companies, and the Norwegian Mapping Authorities. In addition gravity data from satellite altimetry in the deep-water areas have been used (Andersen & Knudsen 1998). The surveys have been levelled using the International Standardization Net 1971 (I.G.S.N. 71) and the Gravity Formula 1980 for normal gravity.*

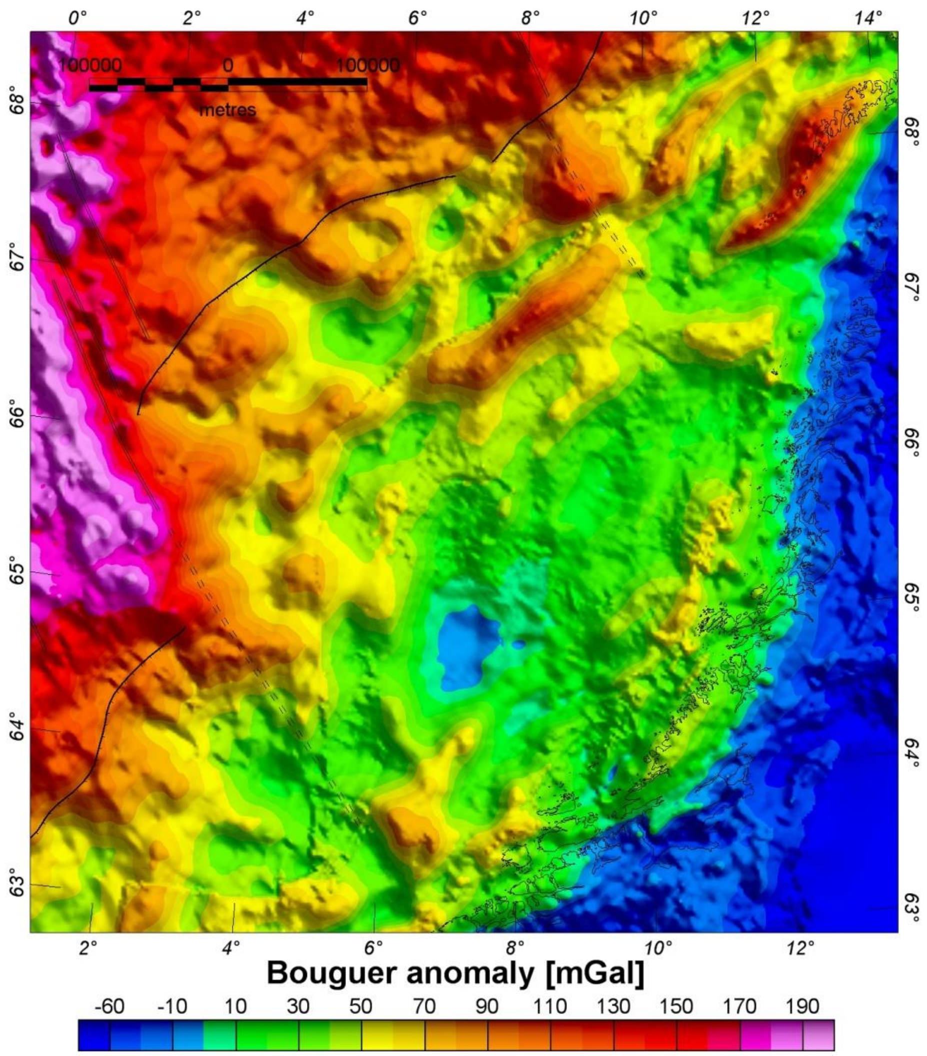

Figure 3.2 *The Bouguer anomaly is calculated using the bathymetry data in Figure 2.2 and an offshore reduction density of 2200 kg/m*^{3}.

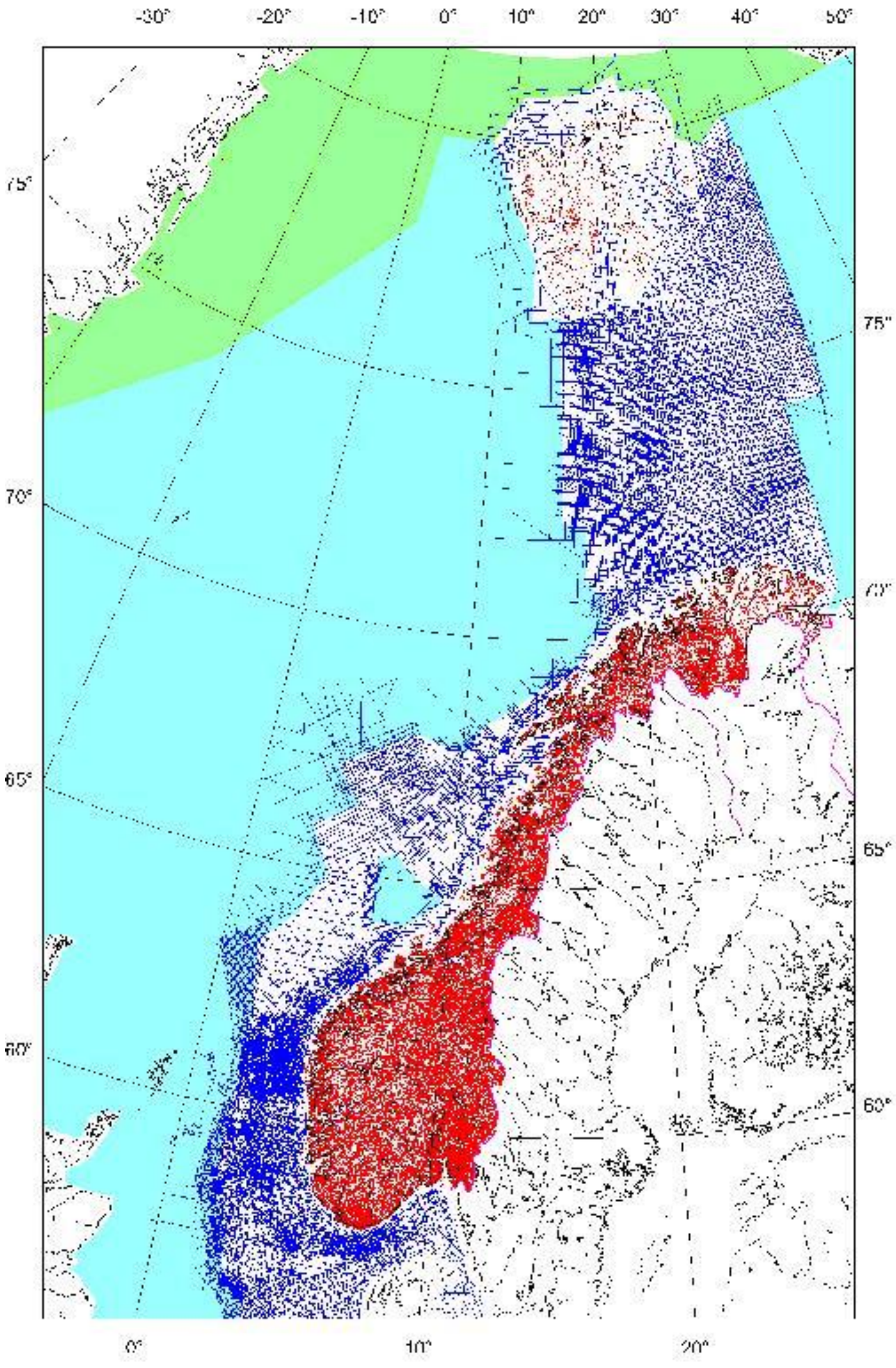

Figure 3.3 *Compilation of gravity surveys in the NE Atlantic (Skilbrei et al. 2000).*

3.2 Aeromagnetic data

The magnetic anomaly (Fig. 3.4) is based on a NGU compilation of different onshore and offshore surveys (Olesen et al. 2006a). Aeromagnetic data from Norway and the adjacent continental margin have been compiled earlier (Skilbrei et al. 1991a; Olesen et al. 1997). The pre-1996 surveys were reprocessed during the periods of 1999-2001 and 2003-2004 using the median levelling and loop closure methods (Mauring et al. 2002, 2003) and these new versions of the NGU-73, Hunting-86, SPA-88, LAS-89, Viking-93 and NAS-94, have been included in the present. Statoil financed parts of this reprocessing within the Dragon database project (DiRect Access to Geophysics On the Net) in 1999/2000. Reprocessed data from the mid-Norwegian continental margin have been published by Olesen et al. (2002, 2004) and Skilbrei et al. (2002) and Skilbrei & Olesen (2005), but the North Sea and Barents Sea datasets remain unpublished. The more recent surveys VGVB-94, MBAM-97, VAS-97, VBE-AM-00 and RAS-03 are also included in the new data compilation.

The offshore aeromagnetic surveys (Fig 3.5) have been gridded to 500 x 500 m cells and added to the regional mainland data compilation. Specifications for these surveys are shown in Table 3.1 The mainland of Norway grid has previously been digitised into a 500x500 m matrix from manually drawn contour maps and the Definite Geomagnetic Reference Field (DGRF) has been subtracted (Nor. geol. unders. 1992). The mainland area was flown at different flight altitudes and line spacing dependent on the topography (Table 3.2). The grids were trimmed to c. 10 km overlap and merged using a minimum curvature algorithm, GRIDKNIT, developed by Geosoft (2005).

Year	Area	Operator	Survey name	Sensor elevation m	Line spacing km	Length km
1973	Vøring Basin	NGU	NGU-73	500	5	6.000
1986	Trøndelag Platform	Hunting	Hunting-86	200	2	57.000
1987	Vøring Plateau	NOO	NOO-87	230	5	16.900
1989	Lofoten	NGU	LAS-89	250	2	24.000
1993	Hel Graben- Nyk High	World Geo-science	SPT-93	80	0.75	19.000
1994	Nordland Ridge-Helgeland Basin	NGU	NAS-94	150	2	28.000
1994	Vøring Basin	Amarok	VGVB-94	140	1-3	31.800
1997	Møre Basin	Amarok/TGS-Nopec	MBAM-97	220	1-2	46.600
1998	Vestfjorden	NGU	VAS-98	150	2	6.000
2000	Southern Gjallar Ridge	TGS-Nopec	VBE-AM-00	130	1-4	17.000
2003	Røst Basin	NGU	RAS-03	230	2	28.000
2005	Jan Mayen FZ	NGU	JAS-05	230	5	32.600

Table 3.1 Offshore aeromagnetic surveys compiled for the present study (Fig. 3.4). NOO - Naval Oceanographic Office; NGU – Geological Survey of Norway; NPD – Norwegian Petroleum Directorate.

Year	Area	Operator	Navigation	Sensor elevation	Line spacing km	Recording
1964	Andøya	NGU	Visual	150 m above ground	1	Analogue
1965	Vesterålen area	NGU	Visual	300 m above ground	2	"
1971-73	Nordland-Troms	NGU	Decca	1000 m above sea level	2	"
1971-1972	Namdalen	NGU	Visual and Decca	300 m above ground	1	"
1959-1969	Central Norway	NGU	Visual	150 m above ground	0.5	"

Table 3.2 Mainland aeromagnetic surveys compiled for the present interpretation.

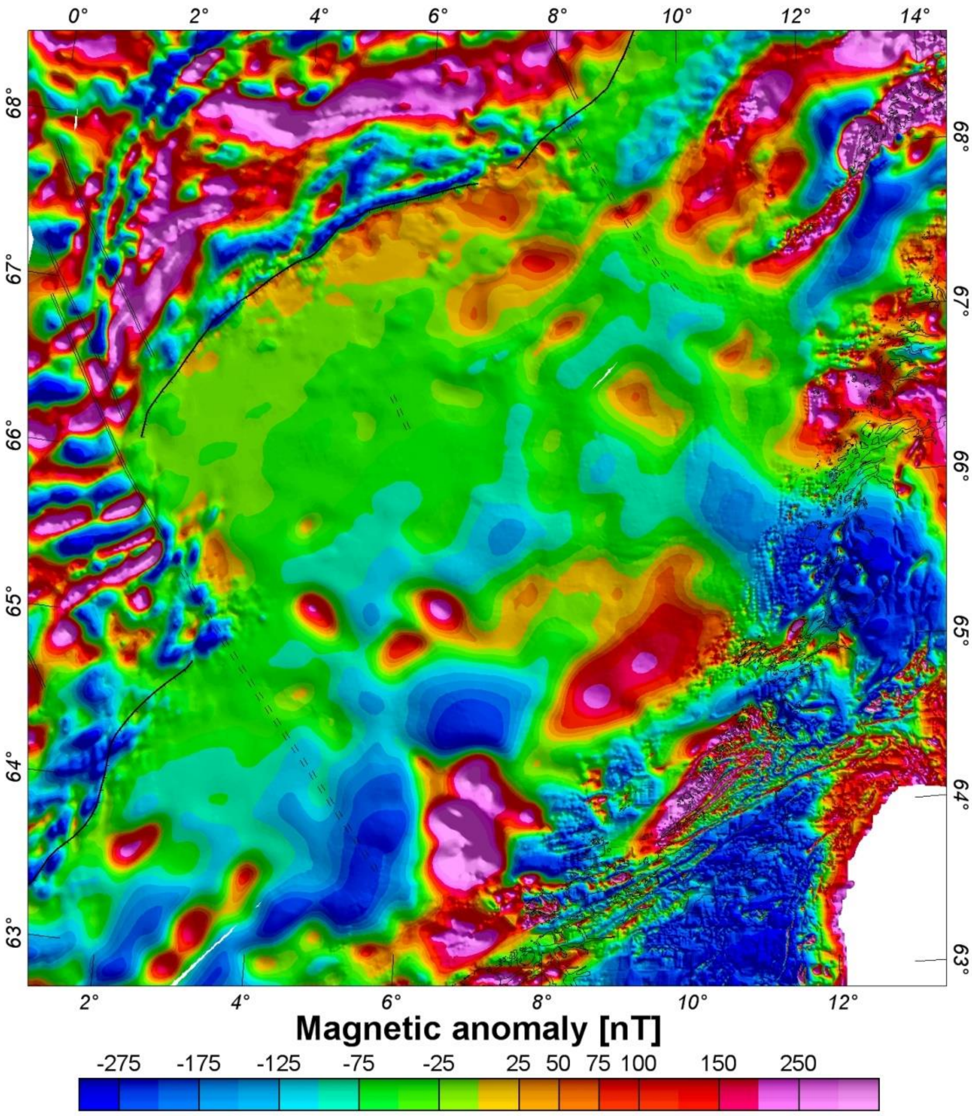

Figure 3.4 *The total magnetic field anomaly is referred to DGRF on the mid-Norwegian continental margin. A total of 12 offshore aeromagnetic surveys have been processed and merged to produce the displayed map (Mauring et al. 2003, Olesen 2002, 2004, 2006a).*

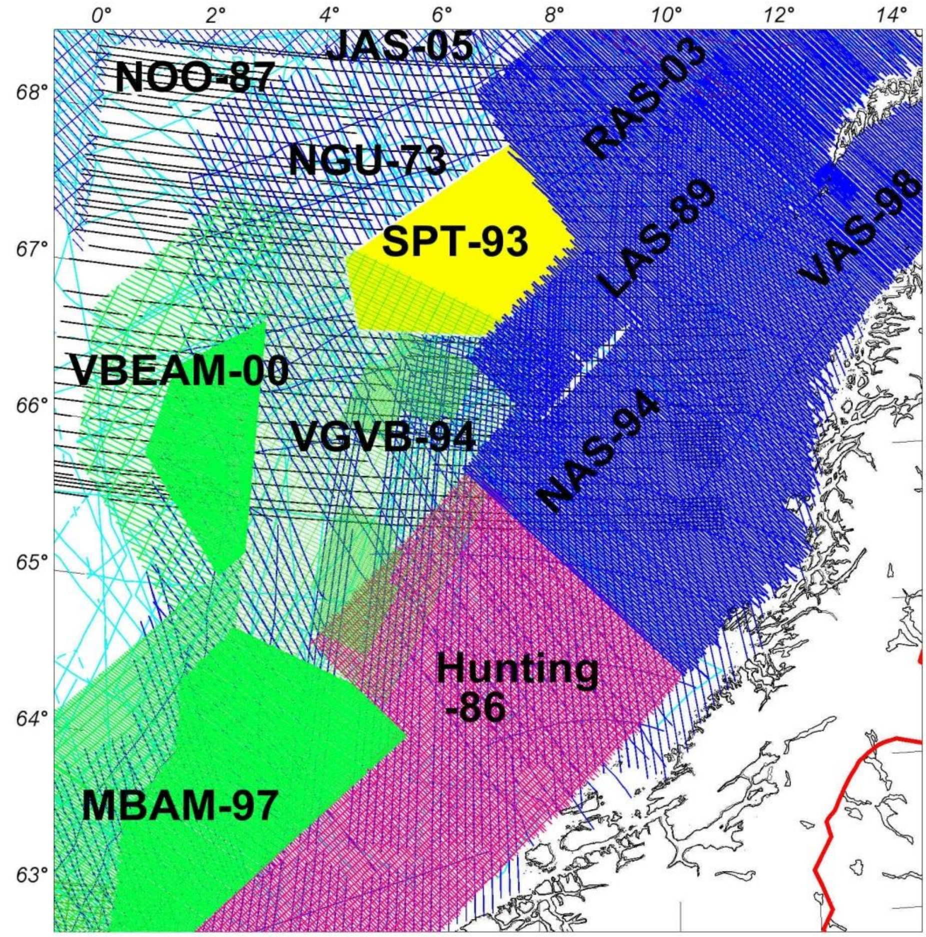

Figure 3.5 *Compilation of magnetic surveys in the Norwegian Sea area. The sub-grids from the aeromagnetic surveys listed in Table 3.1 are produced from original profile data.*

A first comparison of the gravity and magnetic anomalies reveals different structures, probably reflecting sources at different crustal levels. The amplitudes of the magnetic anomalies in the Vøring Basin are very low (around -50±50 nT) and the complex shape of the magnetic anomalies result possibly from changes in bathymetry (distance to near-surface sources), intra-basement variations of magnetic attributes, as well as intrusives (e.g. sills) located at shallower depths within the sediments. Towards the Trøndelag Platform the amplitudes and wavelength of the magnetic anomaly increase, pointing to additional sources in the basement.

3.3 Geometric constraints from seismic data and other sources

Previously, investigations of the mid-Norwegian continental margin have largely been based on interpretation of multi-channel reflection seismic data, refraction seismic data, commercial and scientific drilling, and analysis of potential field data (e.g. Skogseid *et al.* 1992, Doré *et al.* 1999, Brekke 2000, Mjelde *et al.* 2001, Raum *et al.* 2002, Mjelde *et al.* 2003 a, b; Gomez *et al.* 2004, Fernàndez *et al.* 2004, 2005; van Wijk *et al.* 2004). The geometries of the deeper crust and the upper mantle on the mid-Norwegian margin are reasonably well defined by OBS data (see Fig. 2.2 for location). Interpretations of OBS arrays are available from the studies by Mjelde et al. (1992, 1993, 1997, 1998, 2001, 2002, 2003a, 2003b, 2005) and Raum et al.

(2002). In addition, the research group of Rolf Mjelde at UiB provided us with information about the velocity structure along three yet-unpublished OBS transects. These three profiles are especially helpful for our interpretation as two of them cross the Trøndelag Platform and extend onshore, and the third one is located on the Møre margin, where few other regional profiles are available (Fig. 2.2). In addition, the Moho compilation by Kinck et al. (1993) and its modifications by Olesen et al. (2002) have been used to constrain the model in the onshore area.

Our estimate of the offshore basement depth was based on the seismic results mentioned above, plus additional studies by Olesen et al. (1997), Doré et al. (1999), Brekke (2000), Olesen et al. (2002), Osmundsen et al. (2002), and Skilbrei et al. (2002) and Olesen et al. (2004). We have also incorporated the interpretation to depths of magnetic sources (e.g. Skilbrei et al. 2002; Olesen et al. 2004; Skilbrei & Olesen 2005).

We also made use of selected seismic cross-sections that were combined into a series of depth-converted, crustal-scale transects that cross main domain boundaries in the southeastern mid-Norway rift (Figs. 2.1 & 2.2). These transects were compared to the 3D model to constrain the interpretation of the deep basement geometry.

3.3.1 Information from Statoil

Statoil provided gridded data for the area of the Trøndelag Platform:

- Seabed
- Top Paleocene
- Base Tertiary
- Base Cretaceous
- Top Salt
- Top Perm (Fig 3.6)

These grids have a cell size of 500m x 500 m and are based on the interpretation of Statoil internal seismic database. The interpreted horizons were evaluated against the regional seismic lines and used to refine the 3D model of the Trøndelag Platform. An agreement of the 3D modelling and the seismic horizons could be achieved with the exception of the southern Trøndelag Platform (see discussion in Ch. 4).

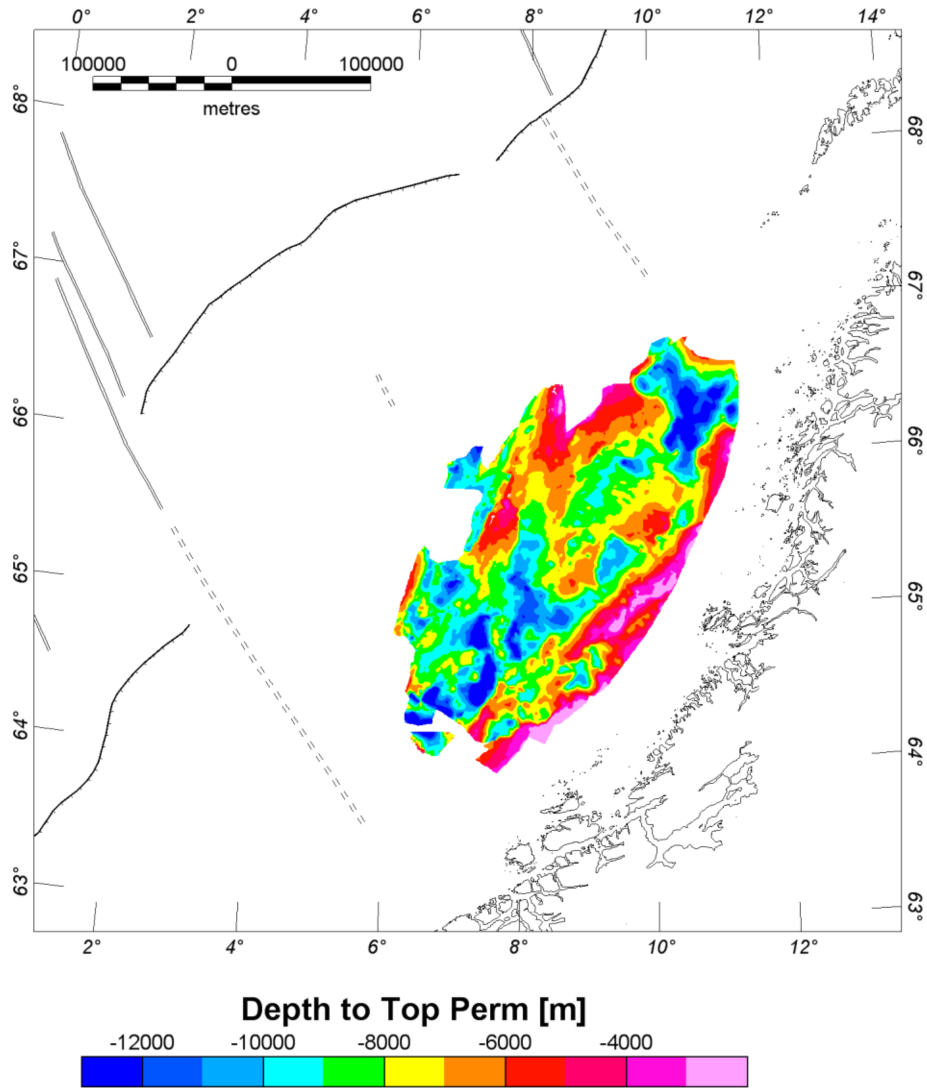

Figure 3.6 *The depth to the top of the Permian as compiled by Statoil. The figure shows also the extent of the provided grid data.*

3.4 Petrophysical information

The two parameters most important for constructing the 3D density and magnetic model are the geometry and the density of the structures. The densities used in the model process are based on published values (Raum et al. 2002, Mjelde et al. 1998, 2001, Olesen et al. 2002, Olesen and Smethurst 1995) and are based on different sources as velocity-density relationships (e.g. Ludwig et al. 1970) or density logs of exploration wells on the Nordland Ridge and Utgard High (e.g. Olesen et al. 2002). The density model values used are shown in Table 5-1. The errors from the velocity-density relations on the applied densities are in the order of ±0.05 Mg/m^3 and ±0.1 Mg/m^3 for the upper basement and deep crustal layers, respectively (Ebbing et al. 2006).

	Raum et al. 2002	**Mjelde et al. 2001**	**Mjelde et al. 1998**	**Olesen et al. 2002**	**Fernàndez et al. 2004**	**this study**
Water	1.03	1.03	1.03	1.03	1.03	**1.03**
Tertiary	1.95-2.25	1.9-2.15	1.95-2.2	2.2	2.2	**2.05-2.1**
Cretaceous Sediments	2.4-2.65		2.45-2.67	2.35-2.5	2.4-2.65	**2.3-2.6**
Upper Cretaceous	265			2.35	2.4	**2.3-2.4**
Lower Cretaceous				2.5	2.58	**2.45-2.55**
Pre Cretaceous	2.68-2.76	2.7-2.81	2.83		<2.6	**2.65-2.7**
Lower Volcanics /Sills		2.62-2.8				
Upper Volcanics		2.7-2.77			2.5	
Cont. Crust	2.82-2.84	2.82-2.9	2.7-2.95	2.75-2.95	2.65-2.95	
Upper Basement						**2.65-2.7**
Lower Basement						**2.75-2.85**
Lower Crust						**2.95-3.0**
LCB	3.0-3.12	3.11-3.22	3.1-3.23	3.1	3.0	**3.1**
Mantle	3.3-3.34	3.33-3.36	3.33	3.25	3.2	**3.3**

Table 3.3 Densities of geological structures in the Norwegian Sea. Density values in Mg/m^3. LCB: lower crustal body.

In general, magnetic anomalies are modelled by applying magnetic parameters to the density modelling. Here, modelling of the magnetic anomalies has been performed, rather on a regional basis for the entire mid-Norwegian margin and more detailed within the Trøndelag Platform. The magnetic parameters we applied to the 3D model are listed in Table 3.4. These parameters are consistent with previous modelling studies in the area (Fichler et al. 1999) and petrophysical measurements (Olesen et al. 1991; Skilbrei et al. 1991b; Mørk et al. 2002).

	susceptibility in SI	**Q-ratio**

Water	0	0
Tertiary Sediments	0.0001	0.4
Other Sediments	0.0002-0.003	0.4
Upper Basement	0.005-0.01	0.5-1.0
Lower Basement	0.02-0.035	0.4-1.1
Lower Crust	0.005	0.5
LCB	0.005-0.0075	0.5
Mantle	0.0025	0.5

Table 3.4 *Magnetic parameters applied in the 3D model. The inclination and declination of all remanent fields is set to 77.0º and 0.5º, approximately parallel to the present magnetic field. For more details see text.*

Most magnetic material is expected to reside within basement rocks (e.g. Fichler et al. 1999), the overlaying sediments making only a small magnetic contribution. Susceptibilities of the basement can range between 0.005 and 0.035 SI (with Königsberg ratios between 0.4-1.1) while susceptibilities of the overlying sediments are in the order of 0.0003 SI (see also 3.4), some two orders of magnitude lower. The upper basement is considered to be less magnetic than the lower basement. (As will be shown later, high-magnetic-intensity basement rocks at shallow crustal levels are related to prominent gravity and magnetic anomalies, especially below the Trøndelag Platform). The main magnetic signature is caused by the changing geometry between the low- and the high-magnetic basement.

Magnetic data will only provide information for the part of the model that presently resides below the Curie temperature. Rocks at higher temperatures will not generate a discernible magnetic signal. Magnetite is regarded to be the dominant magnetic mineral in the region and has a Curie temperature of 580 ºC (cf. Hunt et al. 1995). The depth to the Curie temperature and between magnetic and non-magnetic material runs generally through the lower continental and oceanic crust. Therefore, the upper mantle and the LCB have only a minor contribution to the observed magnetic anomaly.

In previous studies a very shallow depth to Curie temperature has been assumed for the outer Vøring margin (e.g. 12.5 km at the COB, deepening landwards to 22.5 km below the coastline; Fichler et al. 1999, Olesen et al. 2004). This would imply that only the uppermost basement has a contribution to the magnetic field. Recent studies cast some doubts about this assumption (Gernigon et al. 2006a; Olesen et al. 2006b) and therefore the Curie depth is here assumed to be located below the crust. This allows testing the influence of deep-seated sources to the magnetic field.

The geometry of the model is based on the studies described above. The model geometry was derived from the seismic studies described above. These studies constrained the internal geometries of the sedimentary succession, which reduced the uncertainties in the density modelling. Our new interpretation places additional focus on the presence of the basement internal structures (e.g. rotated fault blocks) and their correlation with the gravity and magnetic signal.

4 3D MODELLING

For 3D modelling we utilized the Interactive Gravity and Magnetic Application System (IGMAS; http://www.gravity.uni-kiel.de/igmas). This method calculates the potential field effect of the model by triangulation between modelling planes (Götze & Lahmeyer 1988). The 3D model of the entire mid-Norwegian margin consists of ~40 cross-sections with a spacing of 10-25 km and 26 of these profiles cross the Trøndelag Platform (Fig. 2.2). The varying distance between the cross-sections was chosen to provide good coverage of the main geological features and a good overlay with the OBS and seismic reflection profiles.

The geometry of the models is based on the studies as described above. These studies constrained the internal geometries of the sedimentary succession, which reduced the uncertainties in the density modelling. Our new interpretation focuses further on the presence of basement structures (e.g. rotated fault blocks) and their correlation with gravity and magnetic signal.

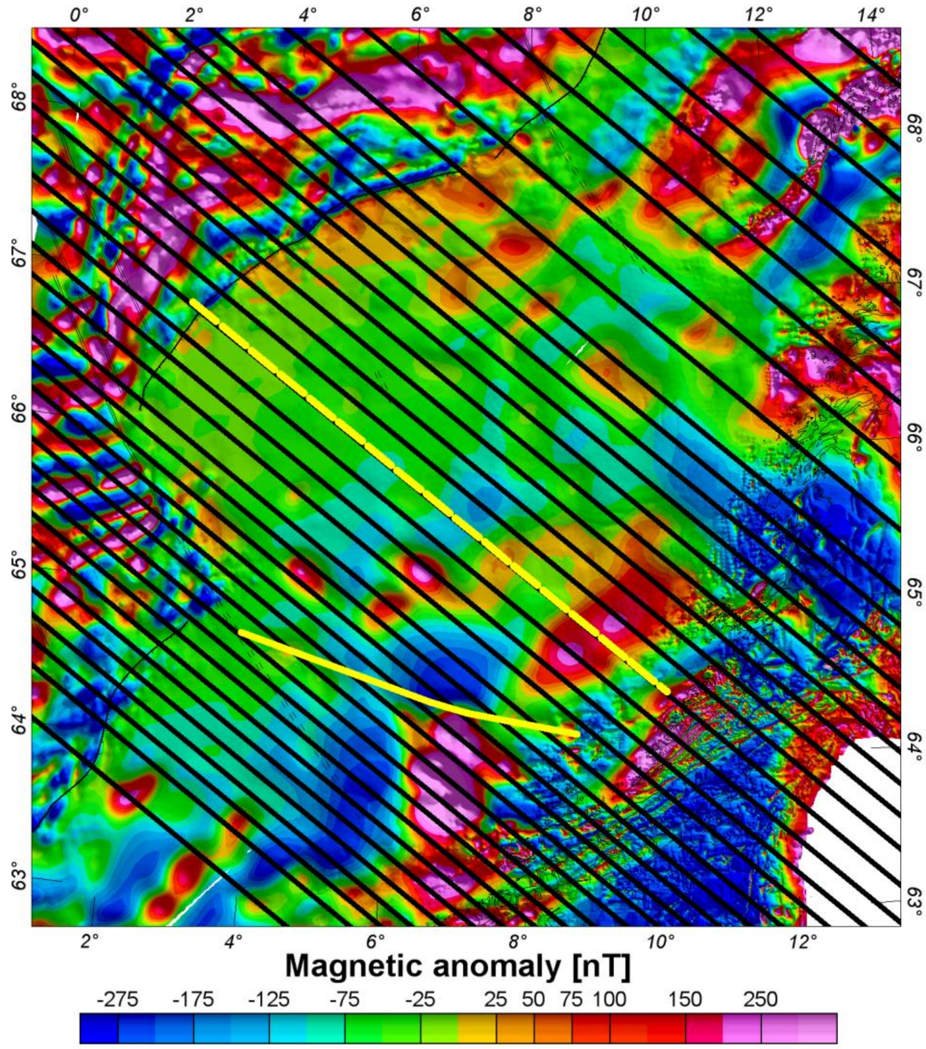

Figure 4.1 *Location of the transects presented in Figures 4.2 (stippled yellow line) and 4.3 (solid yellow line) on top of the magnetic anomaly map.*

Figure 4.1 shows the location of two regional transects crossing the Trøndelag Platform. Figure 4.2 and 4.3 show two cross-sections through the 3D model to demonstrate the geometry of the model. From the 3D model we can extract maps of a variety of surfaces, which again allow a discussion of some structural elements on the mid-Norwegian margin. We will first present depth maps of the key horizons of the model before we discuss maps of crustal/basement thickness.

4.1 Gravity and magnetic response along transects crossing the Trøndelag Platform

The first transect is crossing the central part of the Trøndelag Platform and running from the outer Vøring margin through the Rås Basin and Halten Terrace into the Trøndelag Platform (Fig. 4.2). This transect shows all the characteristics of the crustal structure of the mid-Norwegian margin: very thick sedimentary sequences divided by major domain boundary faults; a thin upper basement underlain by a thick high-magnetic basement, locally cutting through the upper basement; low magnetic anomalies on the outer Vøring margin, but high magnetic anomalies on the Trøndelag Platform; core complexes associated with high magnetic anomalies; a thick high-density lower crustal body on the outer Vøring margin; a flat Moho geometry, rapidly deepening landwards below the Trøndelag Platform. Most of the structures are associated with large density contrasts. A small density contrast (50-100 kg/m^3) occurs between the upper and lower basement only, but a high magnetic contrast exists (Fig. 4.2 a, b). The boundary can also be seen on OBS profiles and partly on long-offset seismic profiles. Modelling of the magnetic anomalies reveals further the importance of the remanent magnetisation for the upper basement. Only induced magnetisation within reasonable magnetic parameters is not sufficient to create the observed magnetic highs. Only with the remanent magnetisation component the magnetic anomalies can be adjusted. The direction of the remanent magnetisation is here modelled to be parallel to the present magnetic field, as observed for high-grade rocks in Lofoten (Olesen et al. 1991) and on the Fosen Peninsula (Skilbrei et al. 1991b).

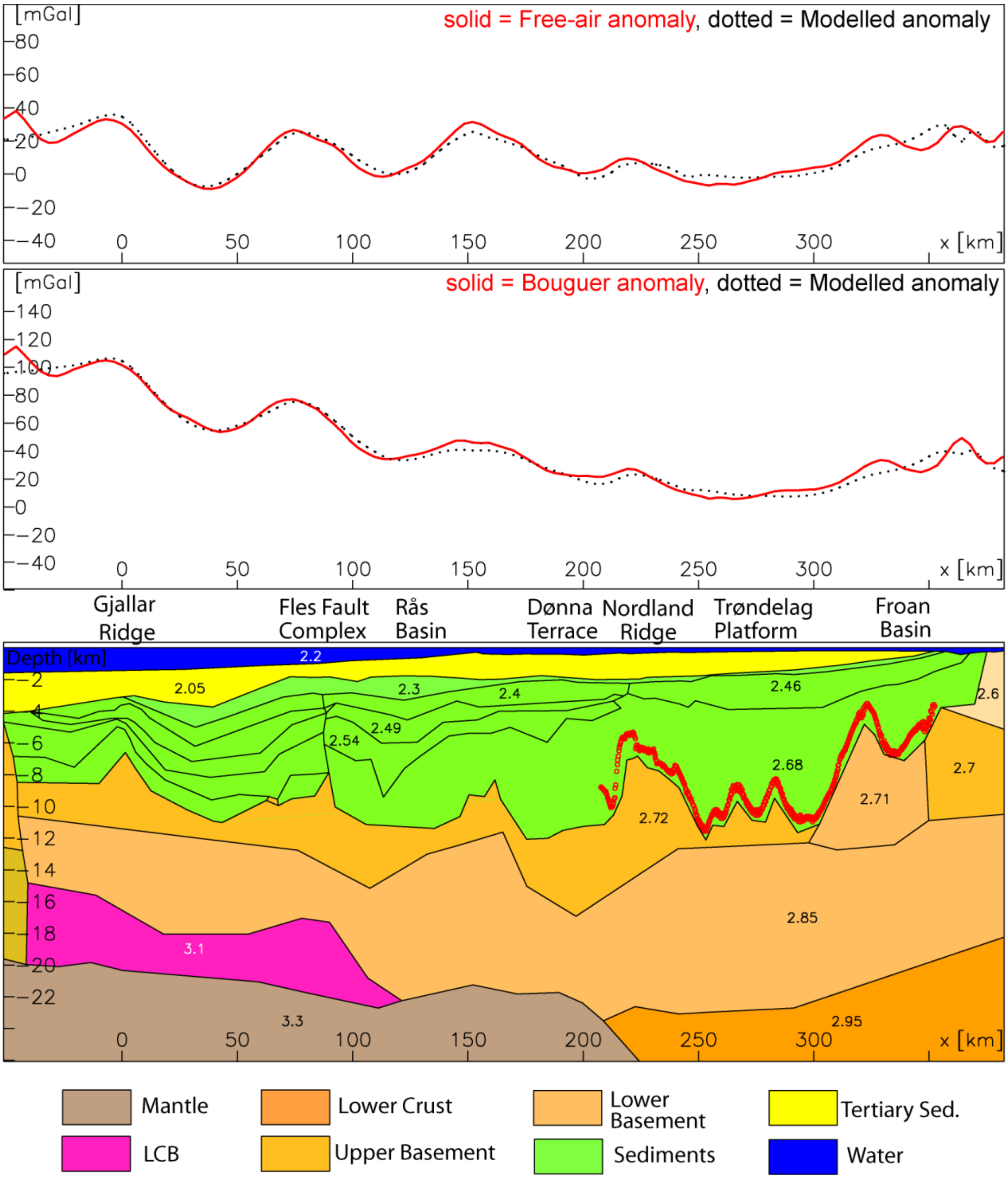

Figure 4.2a *The central transect along the mid-Norwegian margin. The upper panel shows the free air anomaly, the middle panel the Bouguer anomaly. The lower panel shows the modelled density cross-section. Black numbers are density values in Mg/m*^{3}*. The free-air anomaly has been modelled with a water density of 1.03 Mg/m*^{3}**.** *Red line shows the depth to Top Permian from the Statoil compilation. LCB: lower crustal body. See Fig. 4.1 for exact location of the section and text for further details.*

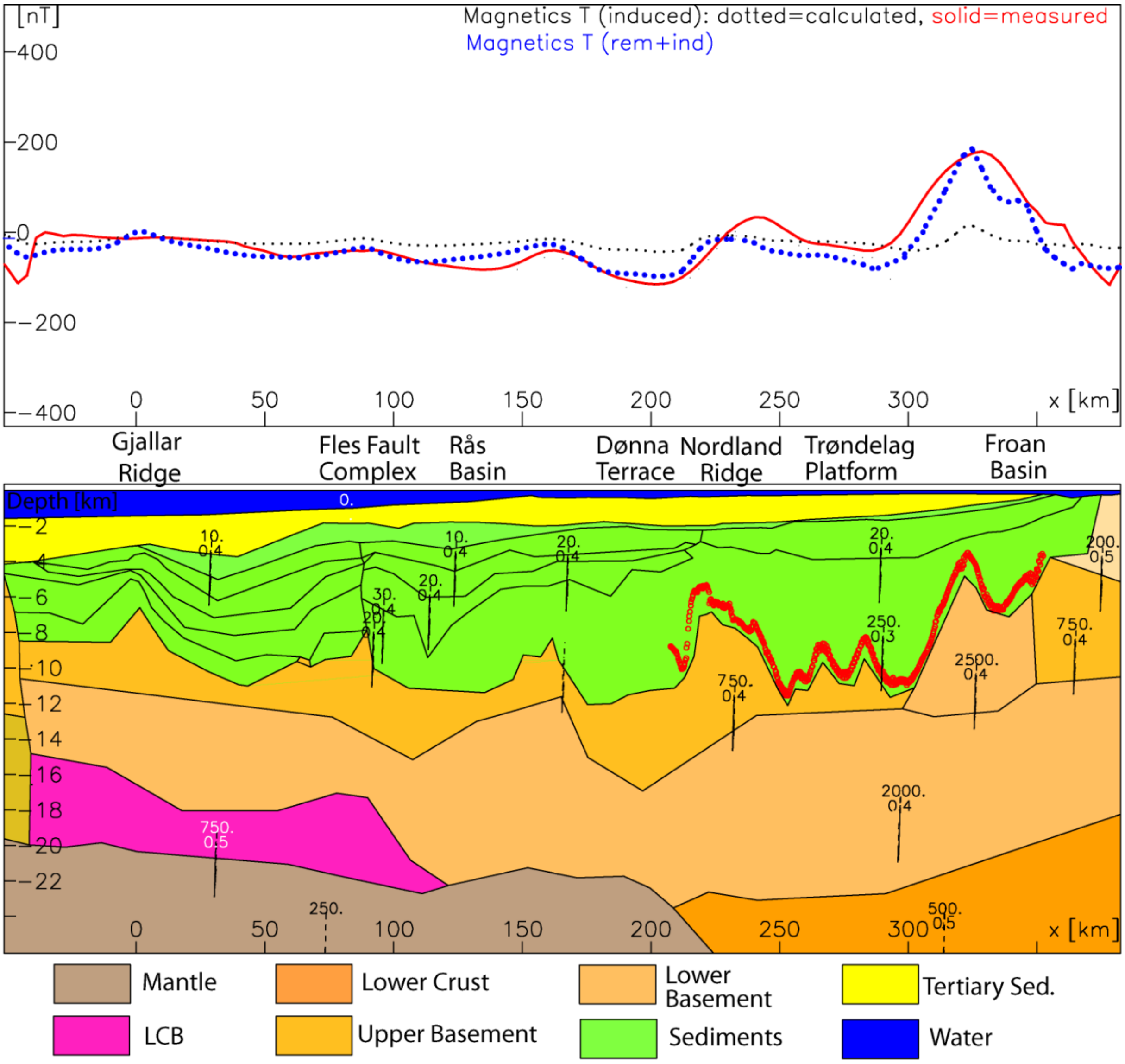

Figure 4.2b *The upper panel shows the induced and remanent magnetic anomalies. The lower panel shows the modelled magnetic properties. Black numbers are magnetic susceptibility in 10^{-5} SI and Q-ratios.*

The second transect is located on the southernmost part of the Vøring Margin, crossing from the Modgunn Arch over the Helland Hansen Arch and Klakk Fault Complex into the Halten Terrace and Froan Basin, along the seismic lines GMNR94-104 and MNT88-08. The free-air gravity anomaly along the profile is varying between +/- 20 mGal and is showing no prominent anomalies. Thus, the signal merely reflects the sediment thickness and the geometry of the Moho. The deepening of the Moho to the east is somewhat compensated by thickening of the lower crust (and thinning of the sediments). The geometry of the western extension of the lower crust can be associated with a fault block. This line location takes also advantage of a thin or absent LCB. Therefore, the line was taken for preliminary thermal modelling and as we can directly study the influence of the basement architecture on the thermal structure and do not have to consider mechanisms for the evolution of the LCB. Again, below the Trøndelag Platform the lower basement can be observed at a shallow depth, cross-cutting the normal upper basement.

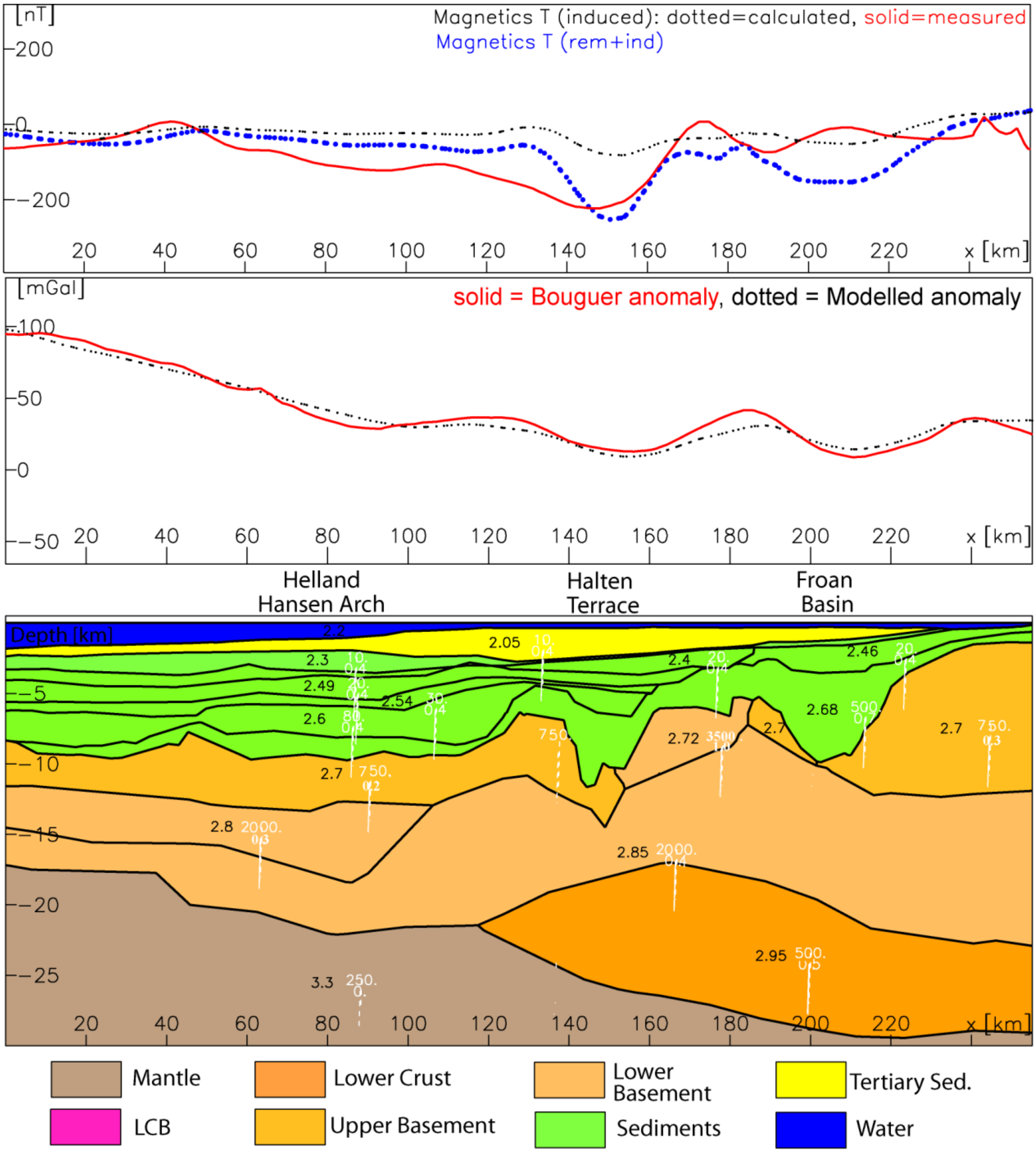

Figure 4.3 *A transect along the profile seismic lines GMNR94-104 and MNT88-08 through the 3D model on the Vøring margin). The upper panel shows the magnetic anomaly, the middle panel the Bouguer anomaly. The lower panel shows the modelled density cross-section. Black numbers are density values in Mg/m*^{3} *and white numbers magnetic susceptibility in 10*$^{-5}$ *SI and Q-ratios.*

The results of the modelling enable us to construct new depth maps of the basement, high-magnetic basement, lower crustal body and Moho for the mid-Norwegian Continental Shelf (Figures 4.4-4.7).

4.2 Upper and lower basement

4.2.1 Upper basement

The map of the top upper basement (Fig. 4.4) reveals a deepening from the coastal area towards the continental margin. The Trøndelag Platform features shallow depths (<9 km), while top basement in the Vøring Basin generally is encountered between 11 and 15 km. The top basement map shows a variety of local features, such as basement highs correlating with the Nyk and Utgard Highs. These structural highs reveal positive gravity anomalies. The depth to the crystalline basement is affected by the basin depth and sediment thickness and the Tertiary domes, especially in the northern Vøring Basin (e.g. Naglfar Dome and Vema Dome). In the southern Vøring Basin the depth to the top basement is similar, but this area lacks prominent basement highs.

The Møre margin to the south also reveals a deep top basement (12-15 km) but the top basement map shows less local features. The East Jan Mayen Fracture Zone marks an approximately 100 km lateral step in the margin. However, the Jan Mayen Lineament is not a well-expressed tectonic feature. Structurally, the transition between the Vøring and Lofoten margins is much more pronounced. Northeast of the Bivrost Lineament the top of the crystalline basement is located at a depth less than 10 km, and obviously reaches the surface on the Lofoten Ridge and at the northern terminations of the Vestfjorden and Ribban Basins. The Bivrost Lineament is a major tectonic boundary marked by both a vertical and apparent horizontal offset. The Utgard and Nyk Highs are suggested to be the southern continuations of the Lofoten Ridge and Røst High, respectively.

On the Trøndelag Platform the depth of the top basement is interpreted with hindsight to the structural interpretation provided by Statoil. The deepest seismic horizon was the Top Perm (Fig. 3.6), which locally exceeded 12 km in depth. At such a depth the density of the sediments is not distinguishable from the underlying basement due to compaction (e.g. Ebbing et al. 2005). Therefore, the depth to the basement was chosen to be deeper than the Permian horizon (except over the Frøya High, as explained below), but a depth estimate of the Permian succession from the density field model has a large degree of uncertainty.

The upper basement can be correlated with the Caledonian nappes as it is less magnetic than the underlying high-magnetic Precambrian basement. Simultaneous modelling of the magnetic and gravity field helps to improve the estimates of the depth to basement, but mainly related to the geometry of the underlying high-magnetic basement.

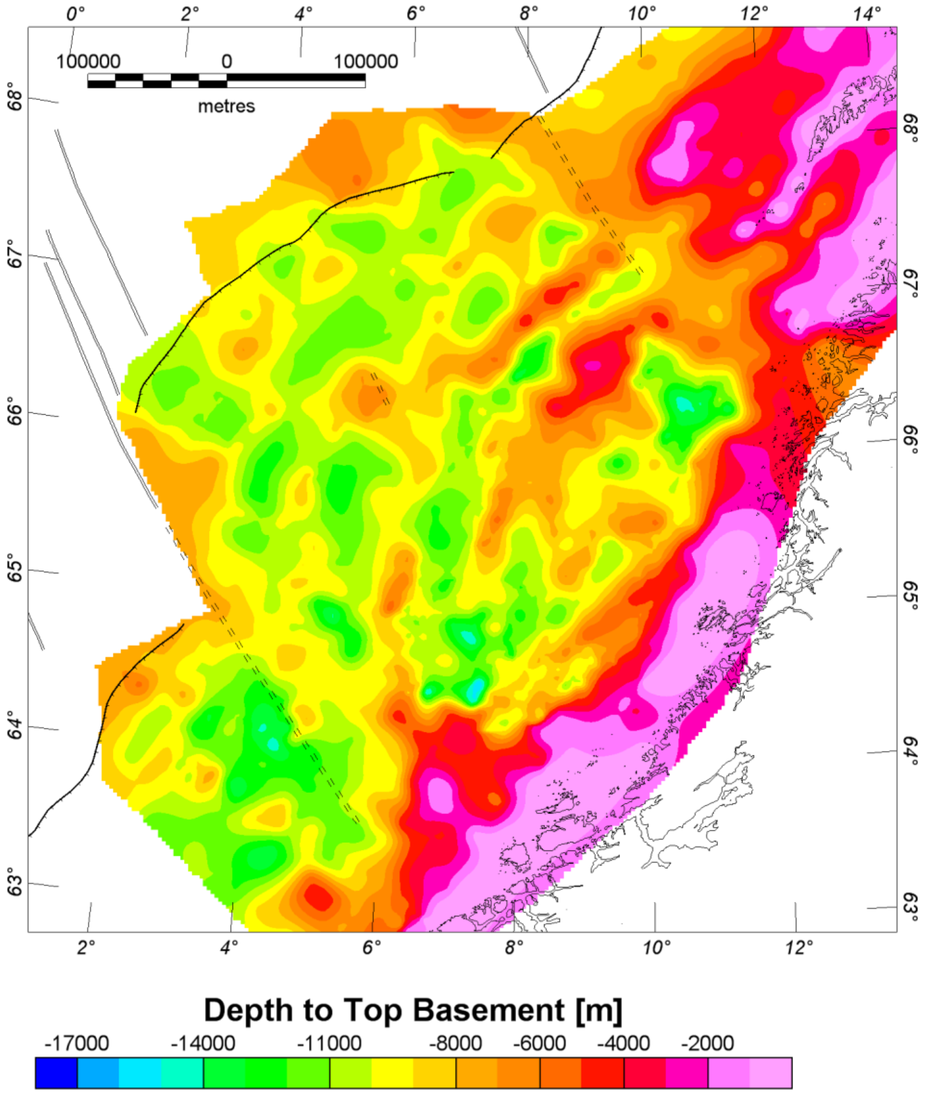

Figure 4.4 *Depth to upper basement. The depth to top basement is associated with the depth to the top of the Caledonian nappes with densities around 2.7 Mg/m3 and relatively low susceptibilities compared to the underlying Precambrian basement (Tables 3.3 and 3.4).*

4.2.2 Lower, high-magnetic basement

The combined seismic and potential field analysis (see below) shows that the lower basement is a key element in the potential field signals on the mid-Norwegian margin, and especially on the Trøndelag Platform. The lower basement is defined to have densities >2.75 Mg/m^3 and higher magnetic properties (Susceptibility of 0.02-0.035 (SI) and Q-ratios up to 1) than the uppermost basement.

The two-division of the basement is also consistent with the velocity structure provided from OBS interpretation (Mjelde et al. 2005, pers. comm.) and the interpretation of the regional seismic lines. On the two transects (Fig. 4.2 and 4.3) a crustal dome (core complex) can be clearly observed which is also correlating with highs (Frøya High). On the magnetic anomaly map (Fig. 3.4) the magnetic high of the Frøya High is clearly extending towards the southern

Halten Terrace. This is in disagreement with the horizons provided by Statoil and our 3D model.

The observed core complex is interpreted to be shallower than the interpretation of the Top Perm. However, the Top Perm grid is not complete in this region and the differences are located at the edge of the available data. The possibility that the core complex is located deeper in the crust is highly unlikely, as the modelling of the core complex already requires high magnetic susceptibility (0.023 SI) and Q-ratio (2.3) for the upper part to adjust the magnetic field. If the core complex would be located deeper, even higher magnetic properties would be required and it would be complicated to model the wavelength of the observed magnetic anomaly. Therefore, the current model appears to be the most reasonable, especially with regard to the potential field signal.

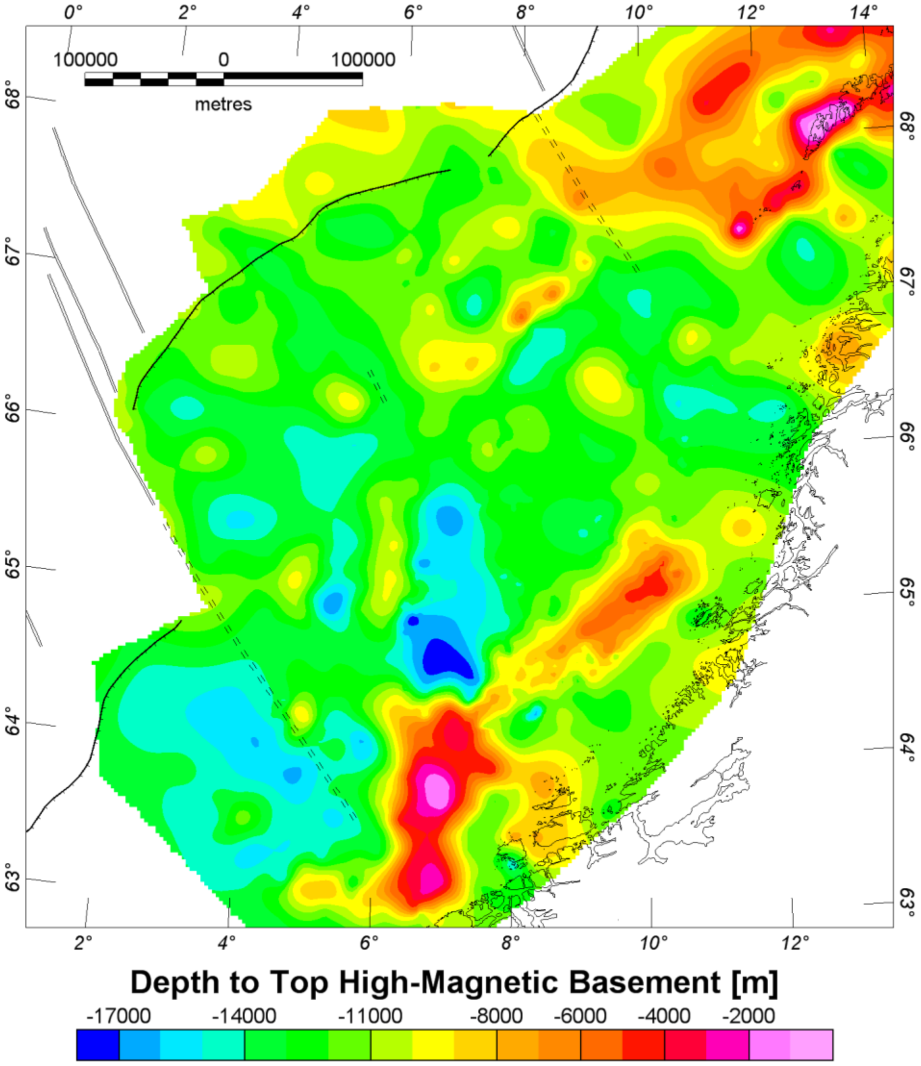

Figure 4.5 *Depth to the lower basement. The lower (Precambrian) basement is defined to have higher densities and magnetic properties compared to the upper (Caledonian) basement.*

4.3 Moho depth and LCB

In addition to the top of the basement the 3D model allows also to model the base of the crust (Moho) and the continental lower crust (CLC) and the lower crustal body (LCB). The interpretation of these horizons is mainly based on the seismic constraints and the density modelling, as the deep part of the crust has only a minor influence on the magnetic field due to the large distance to the source.

4.3.1 Depth to Moho

The depth to the Moho (Fig. 4.6) varies generally between 18 and 28 km. On the Møre margin the depth to the Moho deepens regularly from the coast to the margin, while the Moho depth of the Vøring and Lofoten margins varies more due to local structural features. Overall the central Vøring margin is characterized by a pronounced deep Moho, although the Utgard High is underlain by a shallow Moho, correlating to the shallow Moho below the Lofoten Ridge. Because the Lofoten margin is narrower than the Vøring and Møre margins the shallowing of the Moho is more abrupt.

Below the Trøndelag Platform the Moho is located at a depth of 25 to 30 km. The decrease from the west to east is relatively regular, with the exception of the area between the Froan and Helgeland basins, where the Moho is slightly shallower.

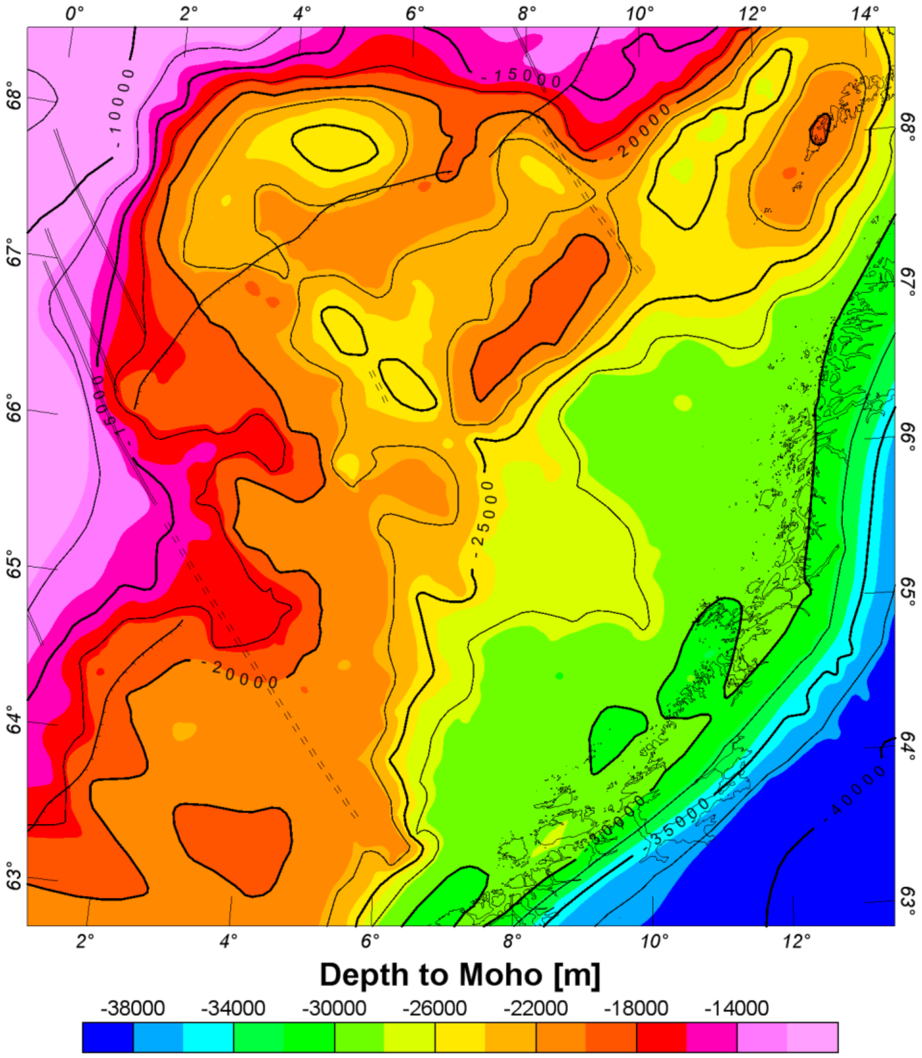

Figure 4.6 *The depth to Moho map clearly shows that the Moho is deepening from a depth of around 20 km to 30 km below the Trøndelag Platform, correlating with the extent of the platform.*

4.3.2 Continental Lower Crust (CLC) and Lower Crustal Body (LCB)

On the innermost part of the mid-Norwegian margin the lowermost crust has increased P-velocities (6.5 km/s) and a density of 2.95-3.0 Mg/m^3. These values are slightly increased from the basement and normal for continental crust. The CLC is located below the Trøndelag Platform and the entire Lofoten margin and is continuing from the margin and eastwards beneath the Scandes (Fig. 4.7), where it is observed in seismic and isostatic studies (Ebbing 2007, Pascal et al. 2007). However, the CLC is not present on the outer margin areas of the Vøring and Møre margin, where the lower crustal body (LCB) can be observed (Figs. 4.7 and 4.8).

The high-density and high-velocity body is located at the base of the crust below large portions of the outer parts of the Mid-Norwegian margin (Fig. 4.8). This lower crustal body (LCB) has a density of around 3100 kg/m^3 and velocities of > 7 km/s. The extension and thickness of the LCB have been mapped in a series of studies (e.g. Mjelde *et al.* 2005; Ebbing *et al.* 2006). While the origin of the LCB remains disputed, its presence is unarguably. For a thorough discussion see Ebbing *et al.* (2006). We consider the LCB to have in general different petrophysical properties than the lower basement.

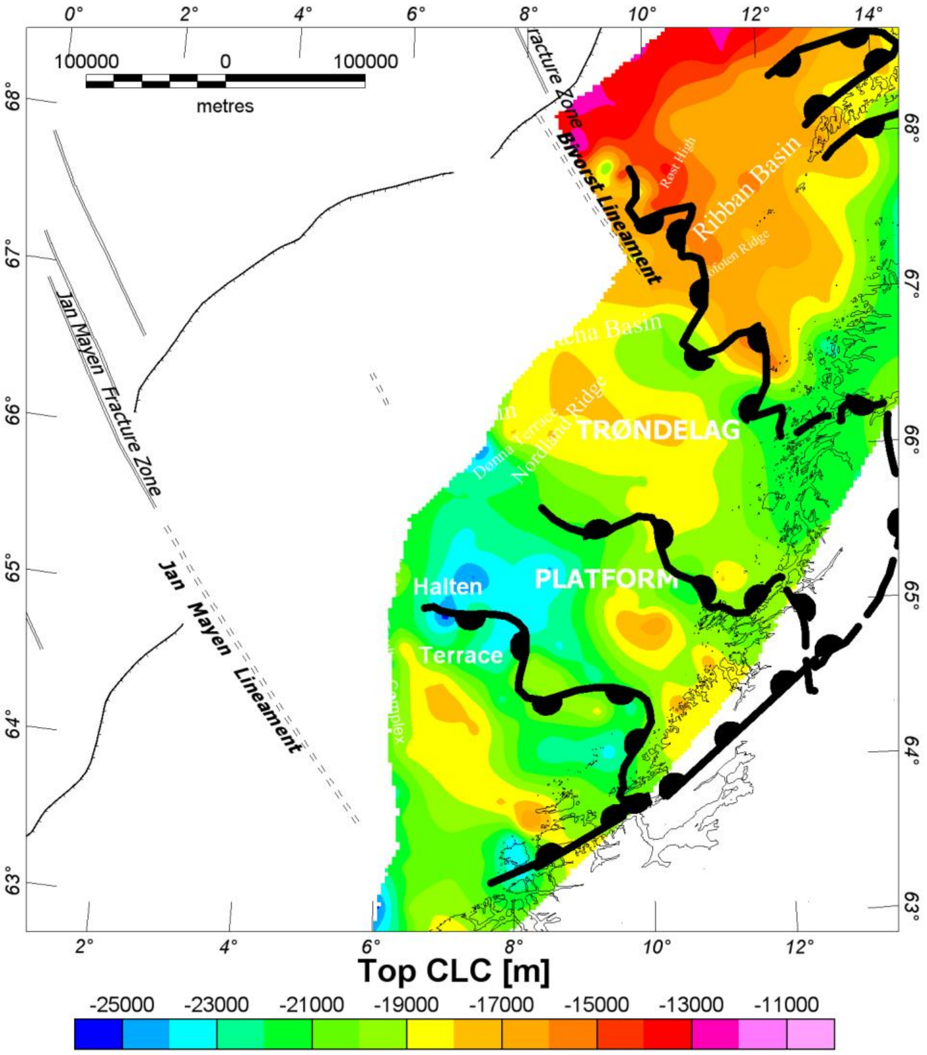

Figure 4.7 *Depth to top of continental lower crust (CLC). The LCB has a density of 2.95-3.0 Mg/m^3 and P-velocities of 6.5-6.9 km/s.*

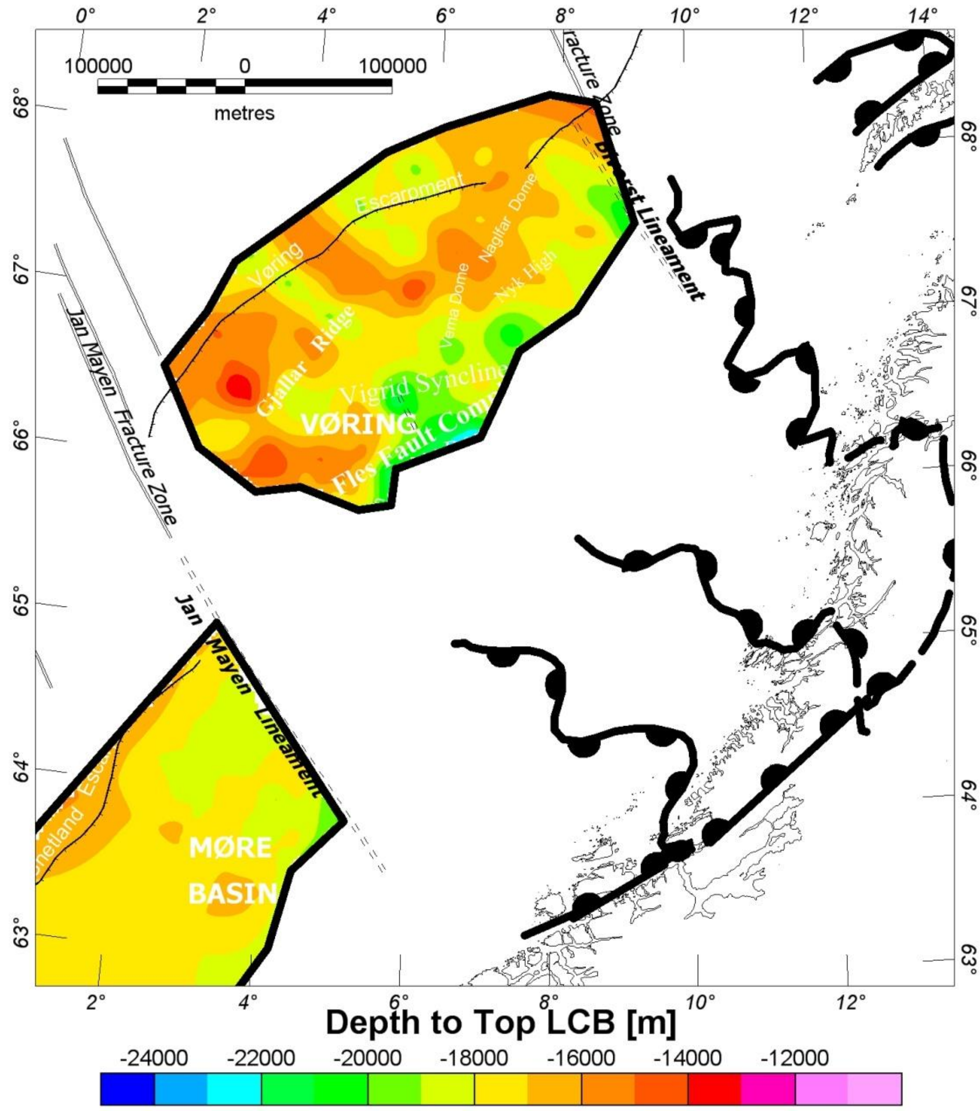

Figure 4.8 *Depth to top of lower crustal body (LCB). The LCB has a density of 3.1 Mg/m³ and P-velocities >7 km/s.*

4.4 Basement thickness

Mapping of the different crustal horizons allows us further to estimate the basement and crustal thickness. Figure 4.9 shows the thickness of the entire crust from the top basement to the Moho.

As mentioned above, the high magnetic basement can be interpreted due to its petrophysical properties to correspond to Precambrian granulite facies whereas the upper, low magnetic basement can be associated to Caledonian nappes and amphibolite facies Precambrian basement.

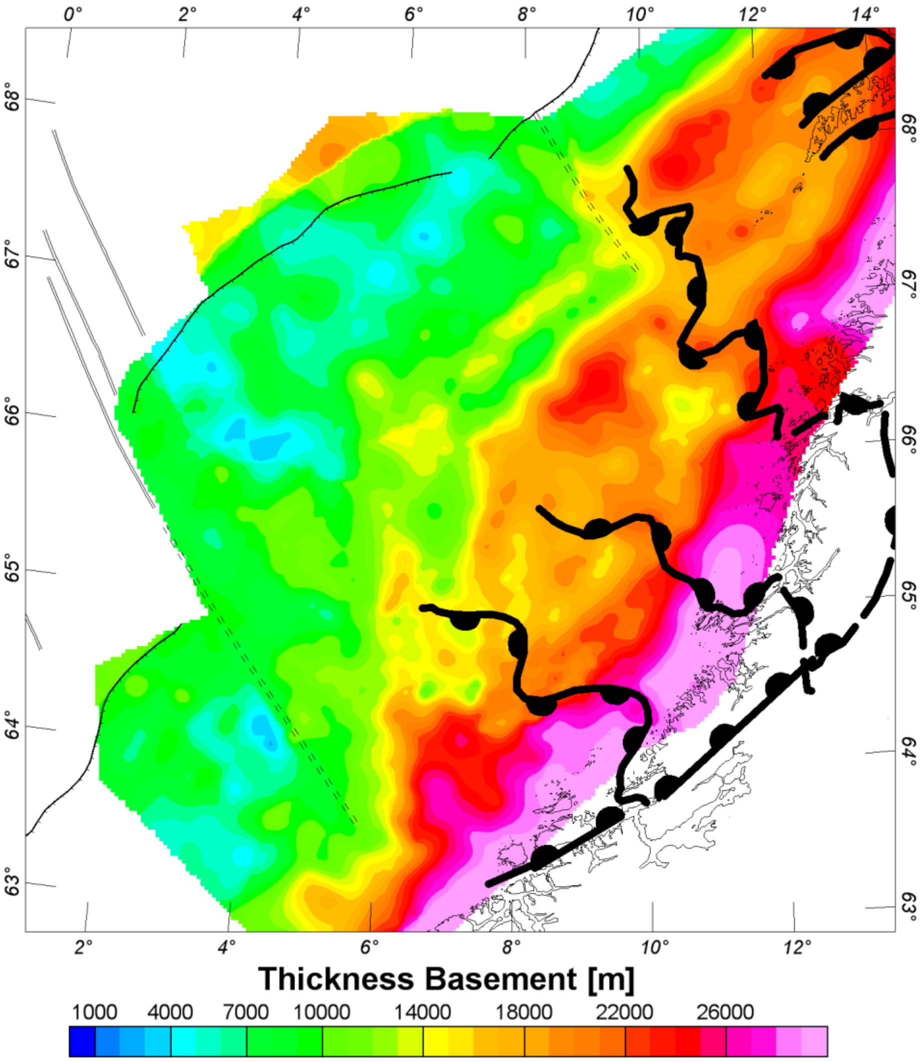

Figure 4.9 *The basement thickness is the entire crustal thickness from the top of the upper basement (Fig. 4.4) to the depth of the Moho (Fig. 4.6). The lateral extend of the lower basement is given by the extent of the 3D density model.*

4.4.1 Thickness upper basement

The upper basement can be associated from its petrophysical properties to be correlating to the Caledonian basement. The thickness map (Fig. 4.10) shows that the Caledonian basement is thickening towards the coastline, but has generally a thickness of 1-3 km on the outer Vøring margin. On the Lofoten margin the upper basement is generally thicker, but has zero thickness on the Lofoten Ridge, where the underlying lower basement is penetrating it. On the Trøndelag Platform the Caledonian basement is also thinning out in the areas of the core complexes.

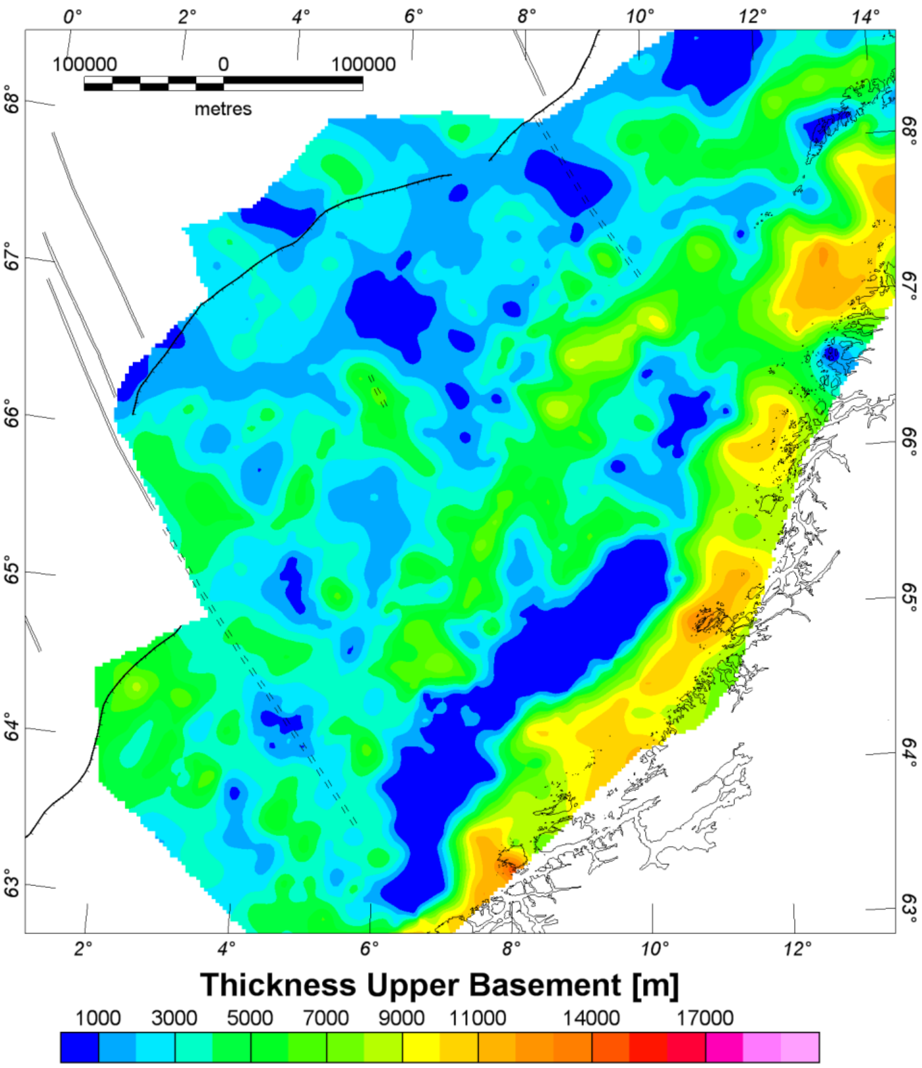

Figure 4.10 *The thickness of the upper basement can be associated with the thickness of the Caledonian basement and is calculated from the top of the upper basement (Fig. 4.4) to the top of the high-magnetic lower basement (Fig. 4.5). The lateral extend of the lower basement is given by the extent of the 3D density model.*

4.4.2 Thickness of lower basement

The thickness of the lower basement is calculated from the top of the lower basement to the Moho. The thickness of the lower basement is roughly correlating with the extent of the Trøndelag Platform (compare Figs. 4.11 and 2.1). However, the isopach map includes the Precambrian portion of the basement, the continental lower crust and the LCB. The thickness of the high-magnetic basement is furthermore correlating surprisingly well with the shape of the magnetic anomalies.

The CLB and the LCB have different petrophysical properties than the Precambrian basement (Table 3.3 and 3.4). Therefore, we have to remove the portion of the CLB and LCB (Fig.4.12) from the thickness of the lower basement (Fig. 4.11) to calculate the correct thickness of the Precambrian, high-magnetic basement (Fig. 4.13). The resulting thickness of the Precambrian basement is correlating less well with the extension of the Trøndelag Platform, but shows a thinning towards the outer margin from 7-12 km below the Trøndelag Platform to less than 6 km on the outer Vøring margin. The thickness of the high-magnetic basement is again correlating with the magnetic anomalies that are especially visible in the areas of the core complexes below the Trøndelag Platform.

The thickness maps indicate that the geometry and thickness of the lower, Precambrian basement is the main element controlling the magnetic anomaly on the mid-Norwegian margin. The Frøya High is an effect of very shallow lower high-magnetic basement and the general presence of a thick magnetic basement. The thickness on the outer Vøring margin is significantly reduced and the magnetic anomaly field is relatively quiet. Consequently, our analysis allows arguing that the relatively low-amplitude magnetic anomalies on the outer Vøring margin are mainly related to the thinning and deepening of high-magnetic material in the basement.

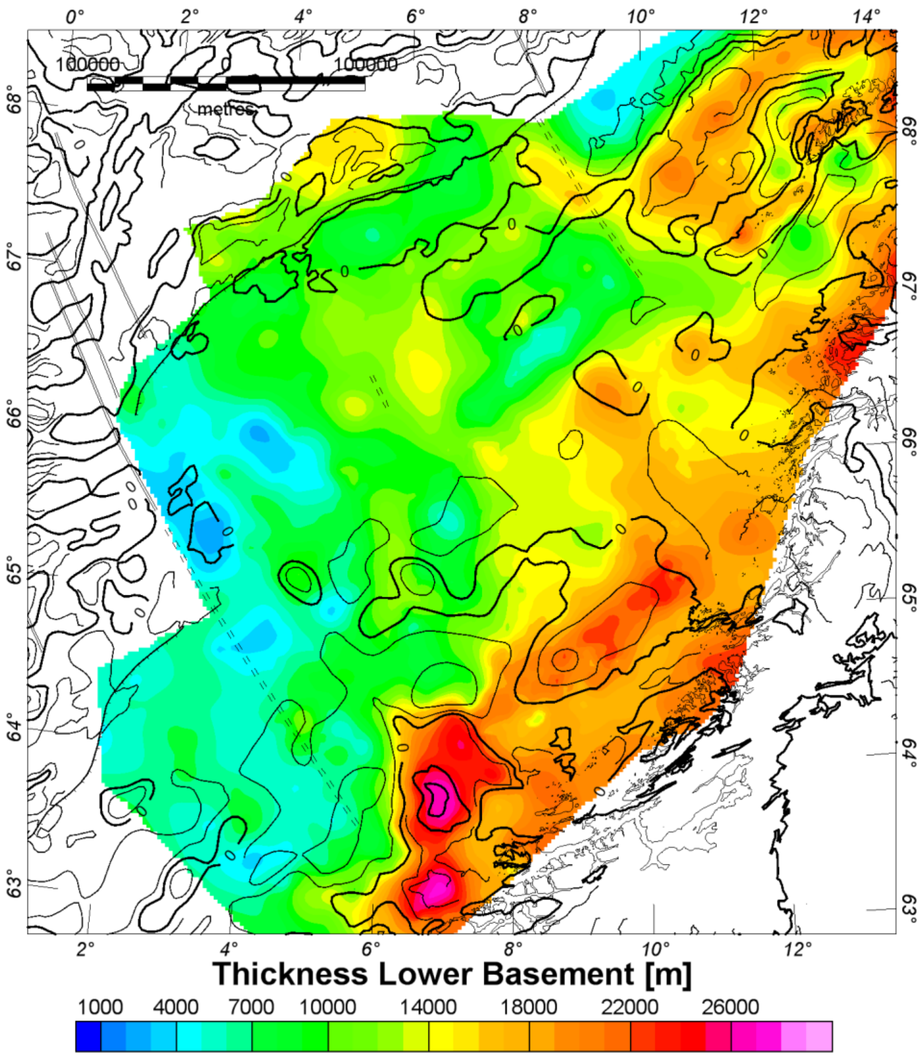

Figure 4.11 *The thickness of the lower basement is calculated from the top of the upper basement (Fig. 4.4) to the Moho (Fig. 4.6) and includes the Precambrian basement and the LCB. The contour lines show the total magnetic field anomaly from Fig. 3.4 (contour distance 100 nT). The lateral extend of the lower basement is given by the extent of the 3D density model.*

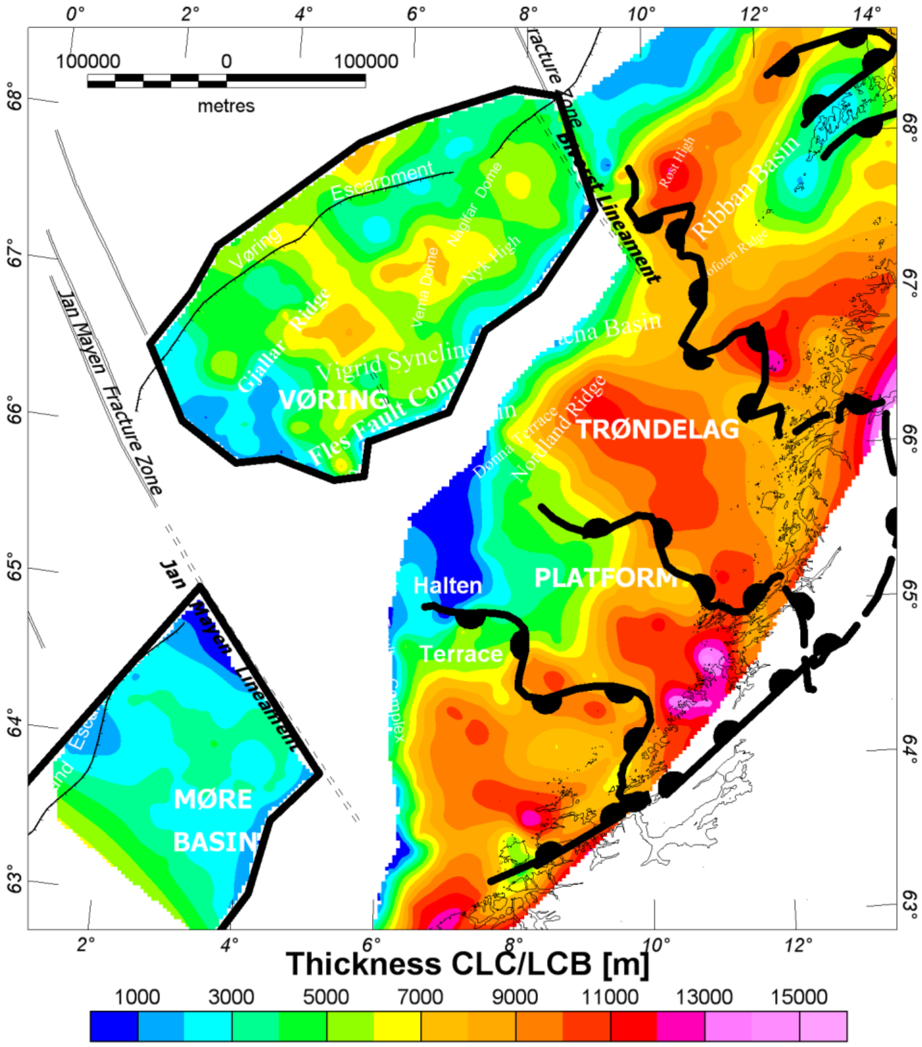

Figure 4.12 *The thickness of the continental lower crust (CLC) and lower crustal body (LCB) is calculated from the top of the CLC and LCB (Figs. 4.7 & 4.8) to the Moho (Fig. 4.6). The lateral extend of the lower basement is given by the extent of the 3D density model.*

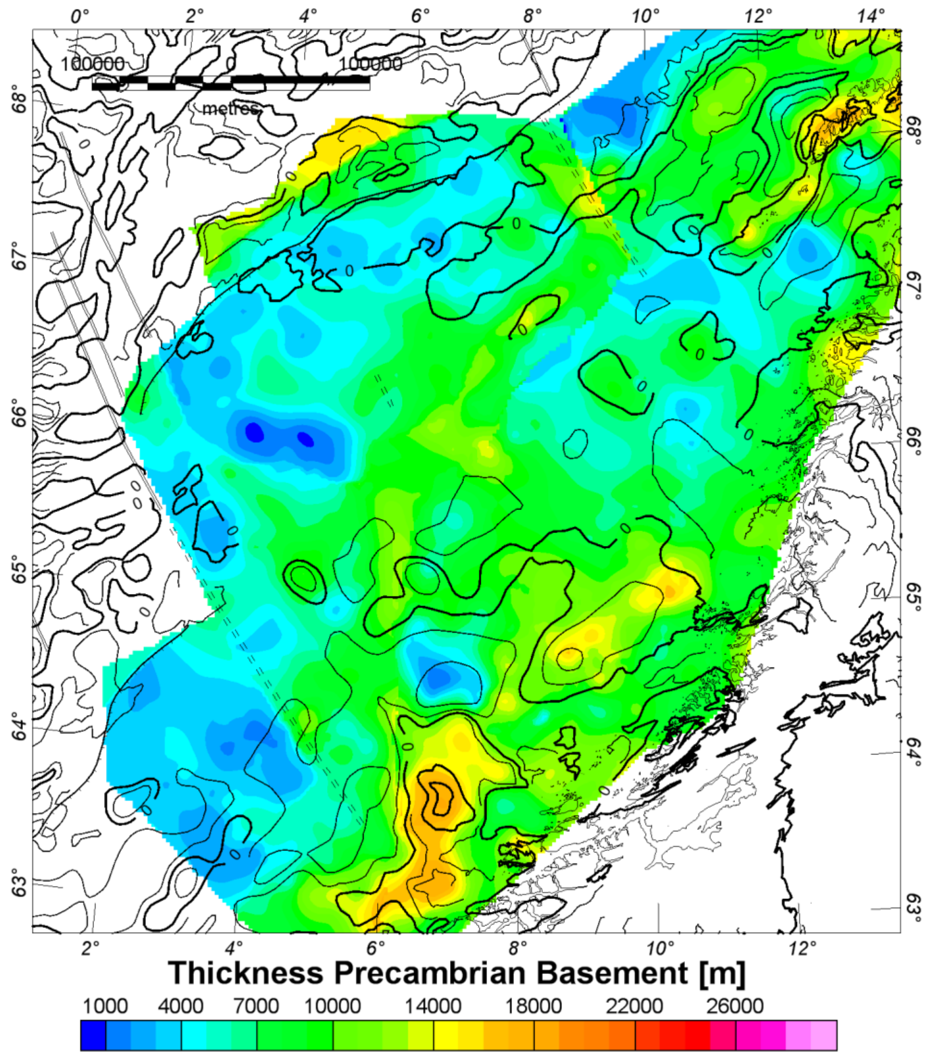

Figure 4.13 *The thickness of the lower, high-magnetic basement is calculated from the top of the upper basement (Fig. 4.4) to the CLC/LCB or Moho (Fig. 4.6, 4.7, 4.8) and includes only the portion of the basement, which can be associated with Precambrian basement. The contour lines show the total magnetic field anomaly from Fig. 3.4 (contour distance 100 nT). The lateral extend of the lower basement is given by the extent of the 3D density model.*

5 TECTONIC SYNTHESIS/INTERPRETATION

Basement

The basement can be subdivided in the upper and lower basement, which are different with regard to their petrophysical properties. The term crystalline basement is avoided in the study, as there exist different meanings of this term. Some studies associate the basement with the crystalline basement (e.g. Christiansson et al. 2000), while others associate it only with the lower basement (e.g. Raum et al. 2002). To avoid confusion with the applied terminology, we use the terms upper and lower basement.

The upper basement has generally lower densities and magnetic properties than the lower basement (Tables 3.3 and 3.4). Comparison to petrophysical sampling onshore Norway allows associating the upper basement with Caledonian nappes and the lower basement with

Precambrian basement (e.g. Olesen et al. 1991). However, the division between the upper and lower basement is not everywhere associated with a clear contrast in density and velocity. However, modelling of the magnetic field anomalies makes a regional mapping of these structures possible. The confidence in the top lower basement estimates is however less than for the upper basement. This is partly due to the large variability of magnetic properties. Petrophysical measurements show large variations in susceptibility and Q-ratio. Further, the direction of the remanent magnetisation is modelled to be parallel to the present magnetic field, but is dependent on the polarity of the magnetic field when the remanent magnetisation was formed.

Our interpretation is constrained by the seismic profiles and we applied magnetic properties that make it reasonable to connect horizons between the seismic profiles. However, the lower basement may feature more complexity in its internal structure than we are able to resolve. Any further interpretation using the depth to high-magnetic basement (Fig. 4.5) and/or the thickness of the lower basement (Figs. 4.11 & 4.13) must consider these uncertainties.

Correlation with onshore structural data

In the Trøndelag Platform area, comparison between seismic and potential field data lend support to previous interpretations of the relationship between positive magnetic anomalies and the offshore continuation of onshore detachment zones. The role of Palaeozoic detachment zones in the denudation of deep, magnetic levels of the crust postulated by previous authors is substantiated by our work. The role of the detachments is especially clear in the thickness and distribution of the continental lower crust (CLC) and the distribution of core complexes.

The Trøndelag Platform: correlation between seismic and potential field data

The distribution and thickness of high-density (>2.75 Mg/m^3) lower crust shows good correlation with the pattern of positive magnetic anomalies in the Trøndelag Platform area. One particularly strong, positive magnetic anomaly in the Central Trøndelag Platform area can be correlated with a doming of the lower crust, interpreted from long-offset seismic reflection data and consistent with our 3D density model. The dome has an amplitude in the order of kilometres and appears associated with crustal thinning along Palaeozoic extensional detachment faults. A deep, NNE-plunging structural culmination underneath the ramp-flat segment of the Bremstein Fault Complex can be traced from the southernmost Halten Terrace into the Frøya High. This correlates well with the strong positive magnetic anomaly that characterises the high, and that crosses the boundary to the Halten Terrace. In the Frøya High, relatively dense basement rocks subcrop sedimentary rocks, consistent with an interpretation of the basement rocks of the Frøya High as originally having belonged to the Caledonian lower crust. Thus, Caledonian lower crust was exhumed in the Frøya High through a combination of post-Caledonian extension and extension related to Mesozoic rifting.

The domain boundary faults and the deep basin areas

Low- to moderate-angle domain boundary faults that separate platform, terrace and subbasin areas from the deep Møre and Vøring basins display geometries consistent with large magnitudes of horizontal separation (10-30 km) and denudation of high-density lower crust in dome-shaped culminations that reside in the footwalls. Osmundsen et al. (2006) interpret the domain boundary faults as main agents in the production of the areas of strongly thinned crust that evolved into deep basins.

Basement structure map

Negative and positive anomalies on the continental shelf reflect to a large extent sedimentary basins and structural highs, respectively. The structural highs on the mid-Norwegian shelf contain high-density and highly magnetised rocks of assumed lower crustal origin and have been interpreted to represent reactivated core complexes (Osmundsen *et al.* 2002, Olesen *et al.* 2002, Skilbrei *et al.* 2002). Figure 5.1 shows the spatial relationship between core complexes, low-angle detachments and the Transscandinavian Igneous Belt (TIB). The lower crustal rocks were exhumed along the low-angle detachments during a late phase of the Caledonian orogeny (Osmundsen *et al.* 2002). It is important to realise that similar core complexes were formed in northern Fennoscandia in the Proterozoic. They are usually referred to as gneiss domes (e.g. Lindroos & Henkel 1978, Midtun 1988, Henkel 1991, Olesen & Sandstad 1993) and are characterized by positive gravity and aeromagnetic anomalies similar to the younger core complexes in mid-Norway. The gneiss domes in northern Fennoscandia were most likely formed during a gravity collapse of the Proterozoic orogen that formed subsequent to continent-continent collision along the Levajok Granulite Belt.

Of particular interest is the recognition of the structurally denuded basement culminations onshore Norway, and their bounding detachments. These major detachments formed during orogen-parallel extension, i.e. at a high angle to the orogenic front (Fig. 5.1). Similar age and style detachments are mapped in East Greenland: the Fjord Region and Ardencaple Detachments (Hartz et al. 2002).

Mapping onshore Norway and East Greenland has revealed the presence of NW-trending Late Caledonian extensional detachments (Braathen et al. 2000: Hartz et al. 2002; Schmidt-Aursch & Jokat 2005 a, b), and it is reasonable to assume that the intervening area, now represented by the offshore parts of the continental margins, was similarly structured (Olesen et al. 2002). Precise correlation between the shear zones in E Greenland and Norway is speculative, however, since the degree of lateral relative motion between the continents during Devonian time remains uncertain. Extrapolating the onshore structures to the offshore realm, it can be deduced that the area outboard Nordland experienced NE-SE trending (i.e. orogen-parallel) late Caledonian gravity collapse. The Kollstraumen Detachment and Nesna and Sagfjord shear zones extend northwestwards below the Helgeland, Vestfjorden and Ribban basins. Downfaulted low-magnetic Caledonian nappes are interpreted to constitute the "basement" southwest of the Bivrost Lineament. Undulations of the offshore extension of the Sagfjord shear zone may have governed the location of the large-scale Mesozoic normal fault zones that bound the sides of the Lofoten and Utrøst Ridges (Olesen et al. 2002).

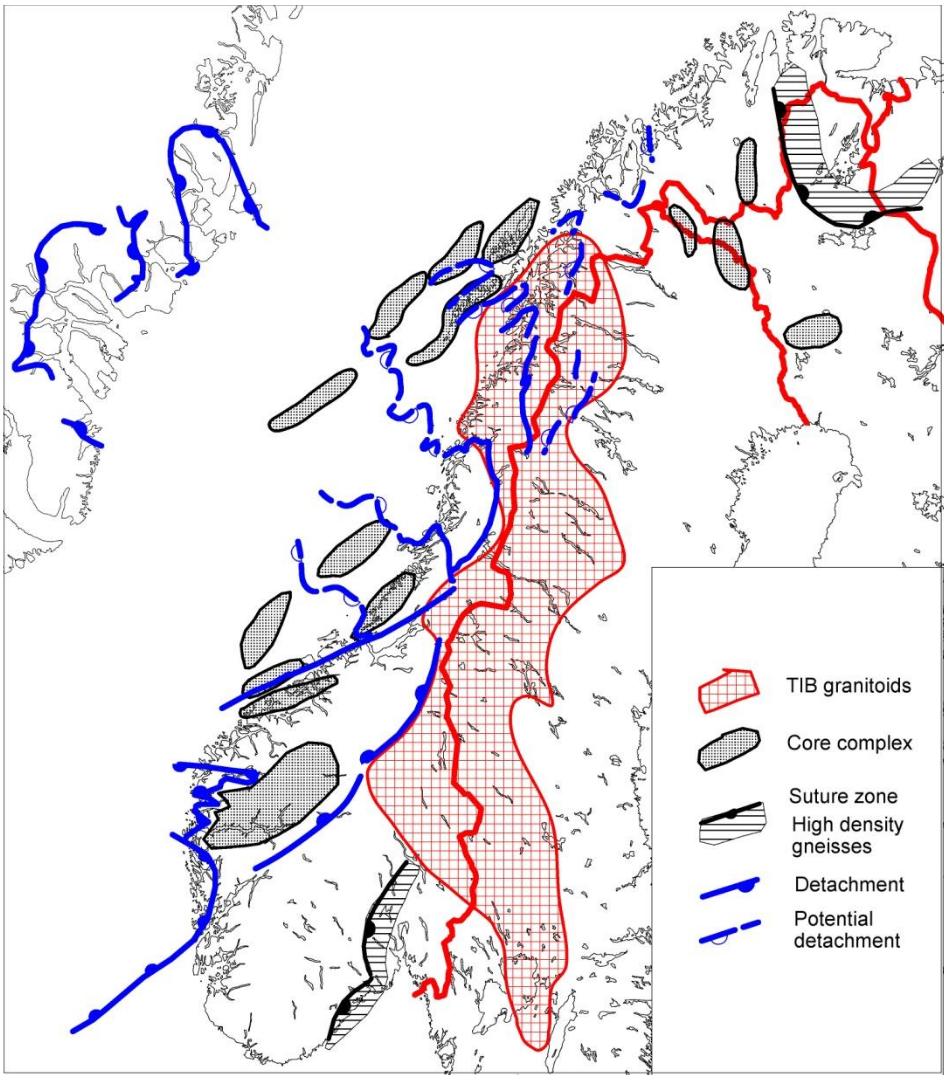

Figure 5.1 *Regional structures compiled from interpretations of potential field data and bedrock mapping (Olesen et al. 2006b). Greenland is rotated back to pre-opening of the Atlantic in the Eocene.*

Lower Crustal body

The LCB in the outer part of the mid-Norwegian margin is one of its most prominent features and it is still under discussion (e.g. Gernigon et al. 2003; Mjelde et al. 2005; Ebbing et al. 2006). Different interpretations exist for this structure and the strong crustal reflectors often associated with it (e.g. Gernigon et al. 2003, Osmundsen et al. 2006). This study is not attempting to address details about the LCB, and we refer to the above-mentioned studies for further details. However, the distribution of the CLC and the LCB allows to question whether the LCB is not generically linked to the CLC. The density and velocity of the LCB is higher than for the CLC, but the spatial distribution allows to argue that the LCB is only a part of the high-grade rocks in the lower crust from the original Caledonian orogeny more affected by extensional and thinning processes of the margin and maybe by some percentage of additional magmatic intrusions.

The origin of the LCB is in any case certainly linked to the palaeo-temperatures on the mid-Norwegian margins. Geodynamic modelling and reconstructions of the Vøring margin must therefore ideally include the LCB (i.e. that the LCB represents magmatically underplated material) since the addition of such material affects the area isostatically (e.g. van Wijk et al 2002). Disregarding the addition of material to the base of the crust leads to underestimation of stretching factors. While dense, the underplated material is lighter than the mantle it replaces and therefore causes uplift. A similar statement can be made for the CLC.

What is generally observed from 2D forward and reverse modelling of profiles is that the mid-Norwegian margin has subsided considerably more than what can be predicted from seismically observable extension (e.g. Roberts et al. 1997). This phenomenon, known as depth dependent stretching, has since become a common observation along passive margins worldwide (Davis and Kusznir 2004). Notably, even if underplating is included or excluded in such modelling, there appears to be a mismatch between subsidence-based stretching factor estimates, those derived from observable faulting, and from whole crustal thinning (Davis & Kusznir 2004).

Curie depth vs. high-magnetic basement

Our analysis allows arguing that the relatively magnetic quietness on the outer Vøring margin is mainly related to the thinning and deepening of high-magnetic basement material. Earlier studies explained the relative magnetic quietness on the outer Vøring margin by a shallow depth to the Curie temperature (e.g. Fichler et al. 1999, Olesen et al. 2003, 2004). Gernigon et al. (2006a) showed that thermal modelling along regional transects leads to temperatures for the lower crust below the Curie temperature of magnetite. They found the 580°C to be located in the uppermost mantle. The comparison shows that a contribution from mantle material to the magnetic signal can be largely excluded.

Strong evidence for the connection of the magnetic anomalies and the lower basement is given by seismic data on the Lofoten margin and the Trøndelag Platform. In both areas the geometry of the high-magnetic basement is clearly related to the high magnetic anomalies and seismic evidence exists for its geometry (e.g. Olesen et al. 2002; Osmundsen et al. 2006).

Along the composite transect GMNR94-104 and MNT88-08 thermal modelling showed that a shallow Curie temperature requires unreasonable high basal heat-flow from the mantle to the crust (Figs. 4.3, 5.2, 5.3; Olesen et al. 2006b). Heat generation values were inferred from onshore measurements assuming that the high magnetic basement corresponds to Precambrian terrains whereas the low magnetic one is associated to Caledonian nappes. Two different models were run with contrasting boundary conditions at their base.

For the first model (Fig. 5.3 left panel), a flat lithosphere base or alternatively a constant Moho heat flow of 40 mW/m^2 was assumed. This first model represents the most conservative one in absence of firm constraints on surface heat flow values. The modelling results in high Moho temperatures (i.e. ~700°C) close to the onshore below the Trøndelag Platform and a relatively steep slope for the isotherms dipping towards the ocean. Predicted surface heat flow values range in between ~50 to ~70 mW/m^2, the highest values being computed for the Trøndelag Platform.

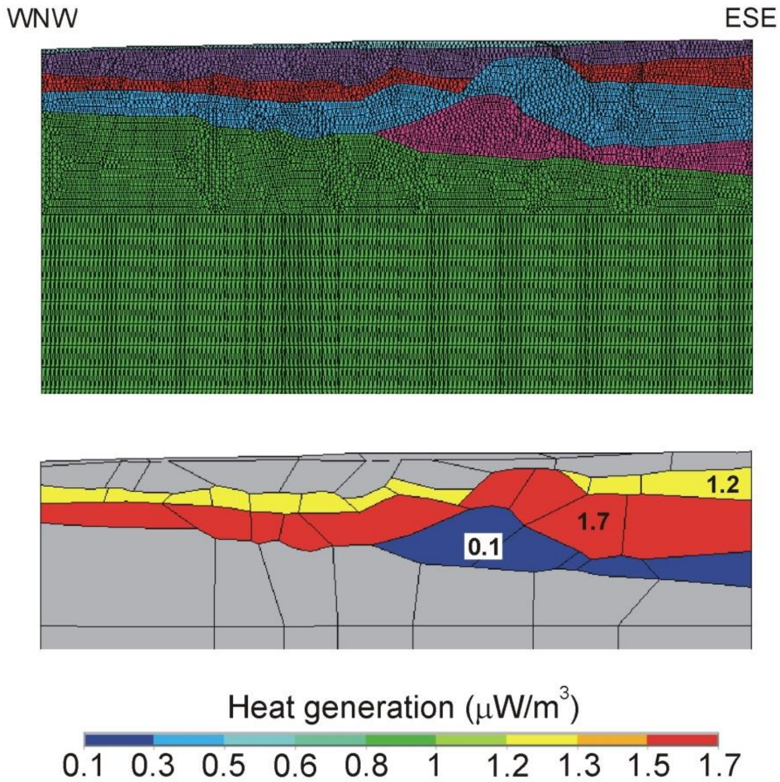

Figure 5.2 *Finite element mesh and heat generation values used for the thermal modelling of the Norwegian Margin Profile (see Fig. 4.3.). Used heat generations for each crustal unit are indicated. Heat generation in the sediments is assumed to be negligible. Conductivities are 1.5, 2.5 and 3.5 W/m/K for Plio-Pleistocene wedges, the crust and the mantle respectively. Boundary conditions are T=0°C at the top and basal heat flow is varied (see text) (taken from Olesen et al. 2006b).*

For the second model, we assumed that the basal heat flow increases gradually from 25 (i.e. cratonic basal heat flow) to 50 mW/m^2 (i.e. old oceanic basin) when travelling from onshore towards the oceanic domain. This model results in lower Moho temperatures, in particular below the Trøndelag Platform (i.e. 600°C). The computed isotherms are almost flat. Interestingly, surface heat flow values vary now between ~50 and ~65 mW/m^2 and show an uneven distribution that is strongly controlled by the structure of the crust.

The calculations for the mid-Norwegian margin show that the influence of different basement lithology might be overprinted by the basal heat flow. Only in the case with a varying basal heat flow the surface heat flow is strongly controlled by the structure of the crust. Here, more effort has to be spent on investigating the change of basal heat flow from the continent-ocean boundary towards the mainland. Correlation with seismic tomography might assist this interpretation as well as detailed analysis of deep crustal structures on the mid-Norwegian margin (correlation between LCB and basal heat flow?).

The presented model shows that it is not required to have a shallow depth to the Curie temperature. Because of the large distance to the sources and the strong dependency of the magnetic field to the source distance, the deep high-magnetic basement has not strong influence on the magnetic field. The observed anomalies on the outer Vøring margin can be associated with the geometry of the top basement. The high-magnetic basement is very thin as the lowermost part of the crust is replaced by the LCB. The LCB is less magnetic than the Precambrian basement, either due to its origin as magmatic underplating and/or as metamorphosed rock (e.g. eclogite). Also, a combination of different effects can be related to the LCB, but, in any case, the properties are different from the Precambrian basement.

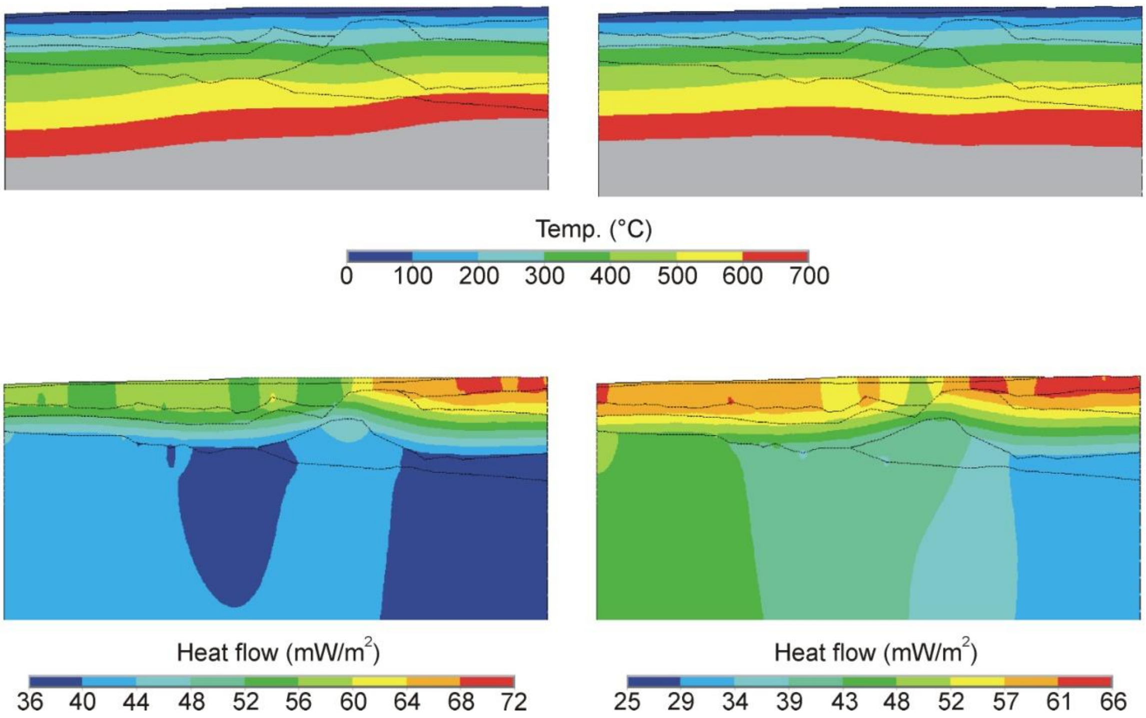

Figure 5.3 *Computed temperature and heat flow values for the Norwegian Margin Profile (taken from Olesen et al. 2006b).*

6 OUTLOOK AND RECOMMENDATION FOR FURTHER WORK

The next step is to use the 3D model, its geometry and the information about the basement, for modelling of thermal state of the entire mid-Norwegian margin. This 3D thermal modelling will be performed in the last stage of the KONTIKI project (Continental Crust and heat Generation in 3D) and will certainly help to evaluate our findings.

The discrepancies in the southern Trøndelag Platform between the 3D model and the delivered seismic horizons should be investigated. The abrupt changes in the geometry of the top basement might explain some differences, as well as the location and spacing of seismic lines. This control can only be done if information about the original seismic data coverage is provided.

The Lofoten and Vøring margin are relatively well studied from a regional perspective and this study fills in with a detailed picture for the Trøndelag Platform. Future studies should extend into the Møre margin, where less information is presently available.

Also the linkage between the offshore mid-Norwegian margin and the Scandes mountains onshore is important to understand the entire passive margin system (e.g. Olesen et al. 2002; 2006b; Ebbing & Olesen 2005; Ebbing et al. 2006; Pascal et al. 2007). The recent Topo-Europe initiative might stimulate integrated onshore-offshore studies that will overcome the discrepancy between the high amount of information available onshore Norway to the relatively poor amount of information about the deep structure on land.

The structural style of the mid-Norwegian margin must further be discussed in the context of the opening of the North Atlantic. Integration with the recent findings of the Jan Mayen Aeromagnetic survey (Gernigon et al. 2006b) and the survey " Norwegian Basin Aeromagnetic Survey" (planned for 2007) will help to answer the questions related to the LCB and the development of the mid-Norwegian margin.

ACKNOWLEDGEMENT

This study was funded by Statoil ASA. We are thankful to Jan Ove Hansen, Kjell Olaf Hartvigsen, Tormod Henningsen, Oddbjørn Kløvjan, Hallstein Lie & Jan Erik Scheie (all at Statoil) for their support and the helpful discussions. We further benefited from the discussions with Laurent Gernigon and Jan Reidar Skilbrei (all at NGU) at some stage about the mid-Norwegian margin. We especially are thankful to Rolf Mjelde (UiB), who provided us with results of the OBS modelling before publication.

REFERENCES

Andersen, O.B. and Knudsen, P., 1998. Gravity anomalies derived from the ERS-1 satellite altimetry. Kort og Martykelstyrelsen, Kopenhagen (www.kms.dk).

Blystad, P., Brekke, H., Fjærsteh, R.B., Larsen, B.T., Skogseid, J. and Tørudbakken, B., 1995. Structural elements of the Norwegian continental shelf. Norwegian petroleum Directorate Bulletin, 8.

Braathen, A., Nordgulen, Ø., Osmundsen, P.T., Andersen, T.B., Solli, A. & Roberts, D. 2000. Orogen-parallel, opposed extension in the Central Norwegian Caledonides. *Geology*, 28, 615-618.

Brekke, H., 2000. The tectonic evolution of the Norwegian Sea continental margin with emphasis on the Vøring and Møre basins. In: Nøttvedt, A. (ed.) Dynamics of the Norwegian Margin. Geological Society of London, Special Publication, 167, 327-378.

Christiansson, P., Faleide, J.I., & Berge, A.M. 2000. Crustal structure in the northern North Sea: an integrated geophysical study. *In:* Nøttvedt, A. (ed) *Dynamics of the Norwegian Margin*, Geological Society of London, Special Publications, 167, 15-40.

Davis, M. & Kusznir, N.J. 2004. Depth-dependent lithospheric stretching at rifted continental margins. *In:* Karner, G.D. (ed.) *Proceedings of NSF Rifted Margins Theoretical Institute*, Columbia University Press, New York, 92-136

Dehls, J.F., Olesen, O., Bungum, H., Hicks, E., Lindholm, C.D. & Riis, F., 2000. Neotectonic map, Norway and adjacent areas 1:3 mill. Norges geologiske undersøkelse, Trondheim, Norway.

Doré, A.G., Lundin, E.R., Jensen, L.N., Birkeland, Ø., Eliassen, P.E. and Fichler, C., 1999. Principal tectonic events in the evolution of the northwest European Atlantic margin. In: Fleet, A.J. and Boldy, S.A.R. (eds.) Petroleum Geology of Northwest Europe: Proceedings of the 5th conference, 41-61. Geological Society, London.

Ebbing, J. 2007. Isostatic density modelling and Neogene reveals the "missing" root of the Scandes. Submitted to Norwegian Journal of Geology, in press.

Ebbing, J. and Olesen, O., 2005. The Northern and Southern Scandes - Structural differences revealed by an analysis of gravity anomalies, the geoid and regional isostasy. *Tectonophysics,* 411, 73-87.

Ebbing, J., Braitenberg, C. and Skilbrei, J.R., 2005. Basement characterisation by regional isostatic methods in the Barents Sea. NGU Report 2005.074, p.78 *Confidential Industry Report.*

Ebbing, J., Lundin, E., Olesen, O. and Hansen, E.K, 2006. The mid-Norwegian margin: A discussion of crustal lineaments, mafic intrusions, and remnants of the Caledonian root by 3D density modelling and structural interpretation. *Journal of the Geological Society, London,* 163, 47-60.

Eldholm, O. and Grue, K., 1994. North Atlantic volcanic margins; dimensions and production rates. JGR, B, 99, 2955-2968.

Fernández, M., Torne, M., Garcia-Castellanos, D., Vergés, J., Wheeler, W. & Karpuz, R. 2004. Deep structure of the Vøring margin: the transition from a continental shield to a young oceanic lithosphere. *Earth and Planetary Science Letters*, 221, 131-144.

Fernández, M., Ayala, C., Torne, M., Vergés, J., Gómez, M. & Karpuz, R., 2005. Lithospheric structure of the Mid-Norwegian Margin: comparison between the Møre and Vøring margins. Geol. Soc. London, 162, 1005-1012.

Fichler, C., Rundhovde, E., Olesen, O., Sæther, B.M., Rueslåtten, H., Lundin, E. and Doré, A.G., 1999. Regional tectonic interpretation of image enhanced gravity and magnetic data covering the Mid-Norwegian shelf and adjacent mainland. Tectonophysics, 306, 183-197.

Gernignon, L., Ringenbach, J.C., Planke, S., Le Gall, B. and Jonquet-Kolstø, H., 2003. Extension, crustal structure and magmatism at the outer Vøring Basin, Norwegian margin. Journal of the Geological Society, London, 160, 197-208.

Gernigon, L., Lucazeau, F., Brigaud, F., Ringenbach, J.C., S., P. & Le Gall, B. 2006a: A moderate melting model for the Vøring margin (Norway) based on structural observations and a thermo-kinematical modeling: Implication for the meaning of the lower crustal bodies. *Tectonophysics 412*, 255-278.

Gernigon, L., Olesen, O., Ebbing, J., Mogaard, J.O., Pascal, C., Wienecke, S., Mondt, J., Norvik, O., Sand, M.and Stehen, Ø., 2006b. Structure of the Jan Mayen Fracture Zone, Norwegian-Greenland Sea - Insights from the New Aeromagnetic Survey JAS-05. EAGE/EAGO/SEG Conference, Saint Petersburg.

Geosoft 2005: Montaj GridKnit, Grid extension for OASIS Montaj v6.1, Tutorial and user guide, *Geosoft Incorporated*, 27 pp.

Gomez, M., Verges, J., Fernandez, M., Torne, M., Ayala, C., Wheeler, W. & Karpuz, R. 2004: extensional geometry of the Mid Norwegian margin before early Tertiary continental breakup. *Marine and Petroleum Geology 21*, 177-194.

Götze, H.-J. and Lahmeyer, B., 1988. Application of three-dimensional interactive modeling in gravity and magnetics. Geophysics, 53(8): 1096-1108.

Hartz, E.H., Eide, E.A., Andresen, A., Midbøe, P., Hodges, K.V., Kristiansen, S.N., 2002. ^{40}Ar/^{39}Ar geochronology and structural analysis: Basin evolution and detrital feedback mechanisms, Hold With Hope region, East Greenland. Nor. Geol. Tidsskr., 82, 341-358.

Henkel, H. 1991: Magnetic crustal structures in Northern Fennoscandia. *In* Wasilewski, P. & Hood, P. (eds.) Magnetic anomalies - land and sea. *Tectonophysics 192*, 57-79.

Hunt, C., Moskowitz, B.M. & Banerje, S.K. 1995: Magnetic properties of rocks and minerals. In: Rock Physics and Phase Relations. A Handbook of Physical Constraints. *AGU Reference Shelf 3*, 189-204.

Kinck, J.J., Husebye, E.S. and Larsson, F.R., 1993. The Moho depth distribution in Fennoscandia and the regional tectonic evolution from Archean to Permian times, Precambrian Research, 64, 23-51.

Lindroos, H. & Henkel, H. 1978: Regional geological and geophysical interpretation of Precambrian structures in Northeastern Sweden. *Sver. geol. unders. C751*, 19 pp.

Ludwig; J.W., Nafe, J.E. and Drake, C.L., 1970. Seismic refraction. In: Maxwell., A. (ed.): The sea, Vo.4, Wiley, New York.

Mathisen, O. 1976: A method for Bouguer reduction with rapid calculation of terrain corrections. *Geographical Survey of Norway geodetic publications 18*, 40 pp.

Mauring, E., Beard, L.P., Kihle, O. & Smethurst, M.A. 2002: A comparison of aeromagnetic levelling techniques with an introduction to median levelling. *Geophysical Prospecting 50*, 43-54.

Mauring, E., Mogaard, J.O. and Olesen, O., 2003. Røst Basin Aeromagnetic Survey 2003 (RAS-03). Ra 3 aeromagnetic compilation. Data acquisition and processing report. NGU Report 2003.070, 20pp.

Midtun, R.D. 1988: Karasjok-grønnsteinsbeltet, Regional geofysisk og geologisk tolkning. *NGU Skrifter 88*, 19 pp.

Mjelde, R., Sellevoll, M.A., Shimamura, H., Iwasaki, T. & Kanazawa, T. 1992. A crustal study off Lofoten, N. Norway, by use of 3D-component Ocean Bottom Seismographs. *Tectonophysics*, 212, 269-288.

Mjelde, R., Sellevoll, M.A., Shimamura, H., Iwasaki, T. & Kanazawa, T. 1993. Crustal structure beneath Lofoten, N. Norway, from vertical incidence and wide-angle seismic data. *Geophysical Journal International*, 114, 116-126.

Mjelde, R., Kodaira, S., Shimamura, H., Kanazawa, T., Shiobara, H., Berg, E.W. and Riise, O., 1997. Crustal structure of the central part of the Vøring Basin, mid-Norway margin, from ocean bottom seismographs. Tectonophysics, 277, 235-257.

Mjelde, R., Digranes, P., Shimamura, H., Shiobara, H., Kodaira, S., Brekke, H., Egjeberg, T., Sørenes, N. & Thorbjørnsen, S., 1998. Crustal structure of the northern part of the Vøring Basin, mid-Norway margin, from wide-angle seismic and gravity data. Tectonophysics, 293, 175-205.

Mjelde, R., Digranes, P., van Schaack, M., Shimamura, H., Shiobara, H., Kodaira, S. & Naess O., 2001. Crustal structure of the outer Vøring Plateau, offshore Norway, from ocean bottom seismic and gravity data. Journal of Geophysical Research, 106, 6769-6791.

Mjelde, R., Kasahara, J., Shimamura, H., Kamimura, A., Kanazawa, T., Kodaira, S., Raum, T. & Shiobara, H. 2002. Lower crustal seismic velocity-anomalies; magmatic underplating or serpentinized peridotite? Evidence from the Vøring Margin, NE Atlantic. *Marine Geophysical Research*, 23, 169-183.

Mjelde, R., Raum, T., Digranes, P., Shimamura, H., Shiobara, H. and Kodaira, S., 2003a. V_p/V_s ratio along the Vøring Margin, NE Atlantic, derived from OBS data: implications on lithology and stress field. Tectonophysics, 369, 175-197.

Mjelde, R., Shimamura, H., Kanazawa, T., Kodaira, S., Raum T. and Shiobara, H., 2003b. Crustal lineaments, distribution of lower crustal intrusives and structural evolution of the Vøring Margin, NE Atlantic; new insight from wide-angle seismic models. Tectonophysics 369, 199-218.

Mjelde, R., Iwasaki, T., Shimamura, H., Kanazawa, T., Kodaira, S., Raum, T. and Shiobara, H., 2003c. Spatial relationship between recent compressional structures and older high-velocity crustal structures; examples from the Vøring Margin, NE Atlantic, and Northern Honshu, Japan. Journal: Journal of Geodynamics, 36-4, 537-562.

Mjelde, R., Raum, T., Breivik, A., Shimamura, H., Mural, Y., Takanami, T. & Faleide, J.I. 2005: Crustal structure of the Vøring margin, NE Atlantic: a review of geological implications based on recent OBS data. In: Doré, A.G., Vining, B.A. (Eds.), *Petroleum Geology: North-West Europe and Global Perspectives - Proceedings of the 6th Petroleum Geology Conference.* Geological Society Special Publication. The Geological Society, London, pp. 803– 813.

Mørk, M.B.E., McEnroe, S.A. & Olesen, O. 2002: Magnetic susceptibility of Mesozoic and Cenozoic sediments off Mid Norway and the role of siderite: implications for interpretation of high-resolution aeromagnetic anomalies. *Marine and Petroleum Geology 19*, 1115-1126.

Norges geologiske undersøkelse, 1992. Aeromagnetisk anomalikart, Norge M 1:1 mill, Norges geologiske undersøkelse, Trondheim.

Olesen, O. & Sandstad, J.S. 1993: Interpretation of the Proterozoic Kautokeino Greenstone Belt, Finnmark, Norway from combined geophysical and geological data. *Nor. geol. unders. Bull. 425*, 41-62.

Olesen, O. and Smethurst, M.A., 1995. NAS-94 interpretation Report, Part III: Combined interpretation of aeromagnetic and gravity data. NGU Report 95.040, 50 pp.

Olesen, O., Henkel, H., Kaada, K. & Tveten, E. 1991: Petrophysical properties of a prograde amphibolite - granulite facies transition zone at Sigerfjord, Vesterålen, Northern Norway. *Tectonophysics 192*, 33-39.

Olesen, O., Torsvik, T.H., Tveten, E., Zwaan, K.B., Løseth, H. and Henningsen, T., 1997. Basement structure of the continental margin in the Lofoten-Lopphavet area, northern Norway: constraints from potential field data, on-land structural mapping and palaeomagnetic data. Norsk Geologisk Tidsskrift, 77, 15-33.

Olesen, O., Lundin, E., Nordgulen, Ø., Osmundsen, P.T., Skilbrei, J.R., Smethurst, M.A., Solli, A., Bugge, T. and Fichler, C., 2002. Bridging the gap between the onshore and offshore geology in Nordland, northern Norway. Norwegian Journal of Geology, 82, 243-262.

Olesen, O., Ebbing, J., Skilbrei, J.R. and Lundin, E., 2003. Interpretation of potential field data along the Lofoten margin, Part 1. NGU Report 2003.089, 68p.

Olesen, O., Ebbing, J., Lundin, E., Skilbrei, J.R., Smethurst, M.A. and Torsvik, T.H., 2004. Interpretation of the Ra 3 potential field data along the Lofoten-Vøring continental margin, Part 2. NGU Report 2004.027, 56p.

Olesen, O., Gernigon, L., Ebbing, J., Mogaard, J.O., Pascal, C. and Wienecke, S., 2006a. Interpretation of aeromagnetic data along the Jan Mayen Fracture Zone: JAS-05. NGU Report 2006.018, p. 161.

Olesen, O., Balling, N., Barrère, C., Breiner, N., Davidsen, B., Ebbing, J., Elvebakk, H., Gernigon, L., Koziel, J., Midttømme, K., Nordgulen, Ø., Olsen, L., Pascal, C., Ramstad, R.K., Rendall, H.O., Rønning, J.S., Skilbrei, J.R., Slagstad, T. and Wissing, B., 2006b. KONTIKI Report 2005-2006, Continental Crust and Heat Generation In 3D. NGU Report 2006.059, p.185.

Osmundsen, P.T., Sommaruga, A., Skilbrei, J.R. and Olesen, O., 2002. Deep structure of the Mid Norway rifted margin. Norwegian Journal of Geology, 82, 205-224.

Osmundsen, P.T., Bøe, R., Davidsen, B., Ebbing, J., Eide, E.A., Hendriks, B.W.H., Redfield, T.F. and Smelror, M., 2006. The recycling of an orogen: provenance and routing of detritus from Norway to the Mid-Norwegian margin. NGU Report 2006.022.

Pascal, C., Ebbing, J. & Skilbrei, J.R., 2007. Interplay between the Scandes and the Transscandinavian Igneous Belt: integrated thermal and potential field modelling of the Central Scandes profile. Submitted to Norwegian Journal of Geology, in press.

Planke, S., Skogseid, J. and Edholm, O., 1991. Crustal structure of Norway, 62° to 70° North. Tectonophysics 189, 91-107.

Raum, T., Mjelde, R., Digranes, P., Shimamura, H., Shiobara, H., Kodaira, S., Haatvedt, G., Sørenes, N. & Thorbjørnsen, T., 2002. Crustal structure of the southern part of the Vøring Basin, mid-Norway, from wide-angle seismic and gravity data. Tectonophysics, 355, 99-126.

Roberts, A. Lundin, E.R. & Kusznir, N.J. 1997. Subsidence of the Vøring Basin and the influence of the Atlantic continental margin. *Journal of the Geological Society, London,* 154, 551-557.

Schmidt-Aursch, M.C. & Jokat, W. 2005a. The crustal structure of central east Greenland - I: From the Caledonian orogen to the Tertiary igneous province. Geophys. J. Int., 160, 736-752.

Schmidt-Aursch, M.C. & Jokat, W. 2005b. The crustal structure of central east Greenland - II: From the Precambrian shield to the recent mid-oceanic ridges. Geophys. J. Int., 160, 753-760.

Skilbrei, J.R. & Olesen, O. 2005: Deep structure of the Mid-Norwegian shelf and onshore-offshore correlations: Insight from potential field data. In: B.T.G. Wandås, E.A. Eide, F. Gradstein, & J.P. Nystuen (Eds), *Onshore-Offshore relationships on the North Atlantic Margin.* Norwegian Petroleum Society (NPF), Special Publication 12. Elsevier, Amsterdam, 43-68.

Skilbrei, J.R., Håbrekke, H., Olesen, O., Kihle, O., Macnab, R. 1991a: Shaded relief aeromagnetic colour map of Norway and the Norwegian-Greenland and Barents seas: Data compilation and examples of interpretation. *NGU Report 91.269,* 15 pp.

Skilbrei, J.R., Skyseth, T. & Olesen, O. 1991b: Petrophysical data and opaque mineralogy of high grade and retrogressed lithologies: Implications for the interpretation of aeromagnetic anomalies in northern Vestranden, Western Gneiss Region, Central Norway. Tectonophysics, 192, p.21-31.

Skilbrei, J.R., Kihle, O., Olesen, O., Gellein, J., Sindre, A., Solheim, D. & Nyland, B. 2000: Gravity anomaly map Norway and adjacent ocean areas, scale 1:3 Million. Geological Survey of Norway, Trondheim.

Skilbrei, J.R., Olesen, O., Osmundsen, P.T., Kihle, O., Aaro, S. and Fjellanger, E., 2002. A study of basement structures and onshore-offshore correlations in Central Norway. Norwegian Journal of Geology, 82, 263-279.

Skogseid, J., Pedersen, T., Eldholm, O. and Larsen, B.T., 1992. Tectonism and magmatism during NE Atlantic continental break-up: the Vøring margin. In: B.C. Story, T. Alabaster and R.J. Plankhurst (Editors), Magmatism and the Causes of Continental Break-up. Geol. Soc. London, Spec. Publ., 68, 305-320.

Smith, W. H. F. & Sandwell, D. T. 1997. Global seafloor topography from satellite altimetry and ship depth soundings. *Science*, 277, 1957-1962.

van Wijk, J.W., van der Meer, R. & Cloetingh, S.A.P.L. 2004. Crustal thickening in an extensional regime: application to the mid-Norwegian Vøring margin. *Tectonophysics*, 387, 217-228.

White, R.S., Spence, G.D., Fowler, S.R., McKenzie, D.P., Westbrook, G.K. & Bowen, N. 1987. Magmatism at rifted continental margins. *Nature*, 330, 439-444.

FIGURES

Figure 2.1 *Tectonic setting of the mid-Norwegian margin (after Blystad et al. 1995).*

Figure 2.2 *Bathymetry of the mid-Norwegian margin. The bathymetric data are from a compilation by Dehls et al. (2000), which is based on satellite altimeter data released by Smith & Sandwell (1997) for the deep-water part of the study are, and data provided by the Norwegian Mapping Authority, Marine Department Stavanger for the shallow water areas. The grey dotted lines in (a) mark the location of the OBS profiles (see Mjelde et al. 2005 for more details), while the thin black lines indicate the cross-sections of the 3D density model. Yellow lines show the long-offset profiles after Osmundsen et al. (2006).*

Figure 3.1 *The gravity anomaly map is a combination of the free-air anomaly offshore and the Bouguer anomaly onshore (modified from Skilbrei et al. 2000). Offshore measurements of approximately 59,000 km of marine gravity profiles have been acquired by the Norwegian Petroleum Directorate, oil companies, and the Norwegian Mapping Authorities. In addition gravity data from satellite altimetry in the deep-water areas have been used (Andersen & Knudsen 1998). The surveys have been levelled using the International Standardization Net 1971 (I.G.S.N. 71) and the Gravity Formula 1980 for normal gravity.*

Figure 3.2 *The Bouguer anomaly is calculated using the bathymetry data in Figure 2.2 and an offshore reduction density of 2200 kg/m^3.*

Figure 3.3 *Compilation of gravity surveys in the NE Atlantic (Skilbrei et al. 2000).*

Figure 3.4 *The total magnetic field anomaly is referred to DGRF on the mid-Norwegian continental margin. A total of 12 offshore aeromagnetic surveys have been processed and merged to produce the displayed map (Mauring et al. 2003, Olesen 2002, 2004, 2006a).*

Figure 3.5 *Compilation of magnetic surveys in the Norwegian Sea area. The sub-grids from the aeromagnetic surveys listed in Table 3.1 are produced from original profile data.*

Figure 3.6 *The depth to the top of the Permian as compiled by Statoil. The figure shows also the extent of the provided grid data.*

Figure 4.1 *Location of the transects presented in Figures 4.2 (stippled yellow line) and 4.3 (solid yellow line) on top of the magnetic anomaly map.*

Figure 4.2a *The central transect along the mid-Norwegian margin. The upper panel shows the free air anomaly, the middle panel the Bouguer anomaly. The lower panel shows the modelled density cross-section. Black numbers are density values in Mg/m^3. The free-air anomaly has been modelled with a water density of 1.03 Mg/m^3. Red line shows the depth to Top Permian from the Statoil compilation. LCB: lower crustal body. See Figure 4.1 for exact location of the section and text for further details.*

Figure 4.2b *The upper panel shows the induced and remanent magnetic anomalies. The lower panel shows the modelled magnetic properties. Black numbers are magnetic susceptibility in 10^{-5} SI and Q-ratios.*

Figure 4.3 *A transect along the profile seismic lines GMNR94-104 and MNT88-08 through the 3D model on the Vøring margin). The upper panel shows the magnetic* *anomaly, the middle panel the Bouguer anomaly. The lower panel shows the modelled density cross-section. Black numbers are density values in Mg/m^3 and white numbers magnetic susceptibility in 10^{-5} SI and Q-ratios.*

Figure 4.4 *Depth to upper basement. The depth to top basement is associated with the depth to the Caledonian nappes with densities around 2.7 Mg/m3 and relatively low susceptibilities compared to the underlying Precambrian basement (Tables 3.3 and 3.4).*

Figure 4.5 *Depth to the lower basement. The lower (Precambrian) basement is defined to have higher densities and magnetic properties compared to the upper (Caledonian) basement.*

Figure 4.6 *The depth to Moho map clearly shows that the Moho is deepening from a depth of around 20 km to 30 km below the Trøndelag Platform, correlating with the extent of the platform.*

Figure 4.7 *Depth to top of continental lower crust (CLC). The LCB has a density of 2.95-3.0 Mg/m^3 and P-velocities of 6.5-6.9 km/s.*

Figure 4.8 *Depth to top of lower crustal body (LCB). The LCB has a density of 3.1 Mg/m^3 and P-velocities >7 km/s.*

Figure 4.9 *The basement thickness is the entire crustal thickness from the top of the upper basement (Fig. 4.4) to the depth of the Moho (Fig. 4.6). The lateral extend of the lower basement is given by the extent of the 3D density model.*

Figure 4.10 *The thickness of the upper basement can be associated with the thickness of the Caledonian basement and is calculated from the top of the upper basement (Fig. 4.4) to the top of the high-magnetic lower basement (Fig. 4.5). The lateral extend of the lower basement is given by the extent of the 3D density model.*

Figure 4.11 *The thickness of the lower basement is calculated from the top of the upper basement (Fig. 4.4) to the Moho (Fig. 4.6) and includes the Precambrian basement and the LCB. The contour lines show the total magnetic field anomaly from Fig. 3.4 (contour distance 100 nT). The lateral extend of the lower basement is given by the extent of the 3D density model.*

Figure 4.12 *The thickness of the continental lower crust (CLC) and lower crustal body (LCB) is calculated from the top of the CLC and LCB (Figs. 4.7 & 4.8) to the Moho (Fig. 4.6). The lateral extend of the lower basement is given by the extent of the 3D density model.*

Figure 4.13 *The thickness of the lower, high-magnetic basement is calculated from the top of the upper basement (Fig. 4.4) to the CLC/LCB or Moho (Fig. 4.6, 4.7, 4.8) and includes only the portion of the basement, which can be associated with Precambrian basement. The contour lines show the total magnetic field anomaly from Fig. 3.4 (contour distance 100 nT). The lateral extend of the lower basement is given by the extent of the 3D density model.*

Figure 5.1 *Regional structures compiled from interpretations of potential field data and bedrock mapping (Olesen et al. 2006b). Greenland is rotated back to pre-opening of the Atlantic in the Eocene.*

Figure 5.2 *Finite element mesh and heat generation values used for the thermal modelling of the Norwegian Margin Profile (see Fig. 4.3.). Used heat generations for each* *crustal unit are indicated. Heat generation in the sediments is assumed to be negligible. Conductivities are 1.5, 2.5 and 3.5 W/m/K for Plio-Pleistocene wedges, the crust and the mantle respectively. Boundary conditions are T=0°C at the top and basal heat flow is varied (see text) (taken from Olesen et al. 2006b).*

Figure 5.3 *Computed temperature and heat flow values for the Norwegian Margin Profile (taken from Olesen et al. 2006b).*